Atmospheric Research 97 (2010) 315–334

Contents lists available at ScienceDirect

Atmospheric Research

journal homepage: www.elsevier.com/locate/atmos

An examination of sensitivity of WRF/Chem predictions to physical parameterizations, horizontal grid spacing, and nesting options

Chris Misenis, Yang Zhang *

North Carolina State University, Raleigh, NC 27695, USA

ARTICLE INFO

Article history:
Received 17 August 2009
Received in revised form 4 February 2010
Accepted 15 April 2010

Keywords:
Meteorological impact on air quality
TexAQS-2000
WRF/Chem
Ozone
$PM_{2.5}$

ABSTRACT

An accurate representation of meteorological processes is important to the accurate predictions of meteorology and air quality. In this study, the Weather Research and Forecasting model with Chemistry (WRF/Chem) is utilized to examine the sensitivity of air quality predictions to two planetary boundary layer (PBL) schemes and three land-surface models (LSMs). Model simulations with different PBL schemes and LSMs are conducted over the Houston–Galveston area for a 5-day summer episode from the 2000 Texas Air Quality Study (TexAQS-2000). Sensitivity to horizontal grid spacing (12 vs. 4 km) and nesting methods (1- or 2-way) is also studied. Model predictions are evaluated with available surface and aircraft observations. Both meteorological and chemical predictions at the surface and aloft show stronger sensitivity to LSMs than to the PBL schemes. The model predictions also show a stronger sensitivity to horizontal grid spacing using 1-way nesting than 2-way nesting and to the nesting method at 4 km than 12 km. The benefits (or disbenefits) of using more complex meteorological schemes, finer horizontal grid spacing, and more sophisticated 2-way nesting may vary and must be evaluated for specific episodes. The results from this study also indicate a need to refine model treatments at a fine grid spacing and the current 2-way nesting method used in WRF/Chem for improvement of model performance.

1. Introduction

Three-dimensional (3-D) atmospheric models are important tools in understanding meteorological variables and their effects on air quality. An accurate representation of meteorological processes is important to the accurate simulation of meteorological variables and chemical species. The planetary boundary layer (PBL) schemes and land-surface models (LSMs) are two important meteorological parameterizations used in 3-D models. As surface-layer variables (e.g., temperature, humidity, wind speed) are simulated within the PBL scheme, they are fed back into the LSM, which simulates outgoing radiation and soil moisture needed by the PBL scheme. The two processes interplay closely, affecting the fate and transport of air pollutants in the PBL. Numerous studies have been conducted on the effects of various PBL and LSM parameterizations on simulated meteorology and atmospheric chemistry (e.g., Pielke, 2001; Bright and Mullen, 2002; Bao et al., 2005; Mao et al., 2006). For example, Chen and Dudhia (2001a) reported that land-surface characteristics and dynamical processes directly influence surface sensible and latent heat fluxes that can in turn alter the structure of the PBL. Holt et al. (2006) found that using an LSM with a better representation of soil transpiration and moisture transport leads to more accurate forecasts of convective precipitation. Zhang et al. (2007) showed that soil, surface, and near-surface temperatures are highly sensitive to LSMs, which in turn affect fine particulate matter ($PM_{2.5}$) and its feedbacks into PBL meteorology.

Both meteorological and chemical processes may be sensitive to horizontal grid spacing and the nesting methods used in the model simulations. Current operational

* Corresponding author. Department of Marine, Earth, and Atmospheric Sciences, Campus Box 8208, NCSU, Raleigh, NC 27606, USA. Tel.: +1 919 515 9688; fax: +1 919 515 7802.
E-mail address: yang_zhang@ncsu.edu (Y. Zhang).

0169-8095/$ – see front matter © 2010 Elsevier B.V. All rights reserved.
doi:10.1016/j.atmosres.2010.04.005

meteorological models typically operate at a horizontal resolution of 12 km (Mass et al., 2002), down from hundreds of kilometers in the late 1950s. Models currently under development and slated for operational use within the next few years are designed to operate at even finer resolution (e.g., the Weather Research and Forecasting (WRF) model at 1 to 10 km (Michalakes et al., 2001)). As compared with that at coarser grid spacing, model performance using finer horizontal spacing may be better, worse, or similar, due to uncertainties in the performance of various physical parameterizations and the complexity in chemistry and meteorology and the non-linear interactions between chemistry and meteorology and their responses to grid resolution (Jang et al., 1995; Zhang et al., 2006a, b; Wu et al., 2008; Queen and Zhang, 2008). While several studies reported that increasing grid resolution may lead to better reproduction of fine-scale meteorological processes (e.g., Mass et al. (2002); Jimenez et al. (2006); Liu and Westphal (2001)), this may not necessarily correlate to better model accuracy (Gego et al., 2005). While Mathur et al. (2005) reported an improved agreement of simulated surface O_3 mixing ratios with observations with an increased grid resolution over North Carolina, Arunachalam et al. (2006) and Wu et al. (2008) showed similar O_3 performance at 4 and 12 km. In contrast with simulated O_3, $PM_{2.5}$, and some $PM_{2.5}$ species such as NH_4^+, simulated precipitation and wet deposition amounts are quite sensitive to horizontal grid spacing (Queen and Zhang, 2008).

In addition to simply decreasing the horizontal grid spacing, 3-D models also use nesting techniques (i.e., 1- and 2-way). 1-way nesting uses the output of a coarser grid simulation as input for the finer grid simulation. Two-way nesting involves feedback from the fine domain to the coarse domain and vice versa. The use of nesting enables the simulation of feedbacks among various meteorological and chemical processes occurring at various temporal and spatial scales. Some studies have shown that using nested domains can lead to more accurate predictions of chemical species (Gego et al., 2005; Fast et al., 2006).

In this study, an online-coupled meteorology and chemistry model, i.e., the WRF model with chemistry (WRF/Chem) (Grell et al., 2005) has been used to simulate a 5-day episode from the 2000 Texas Air Quality Study (TexAQS-2000) over the Houston–Galveston area in Texas (TX). In light of large sensitivities to model physics options and configurations reported by previous studies, a number of sensitivity simulations are conducted. Such sensitivity simulations are particularly important to WRF/Chem, as it is a relatively new model that is being developed by the scientific community and that has not been extensively evaluated. The objectives are to examine the sensitivity of simulated meteorology and air quality to three PBL schemes, two LSMs, two horizontal grid spacing (4 vs. 12 km), and two nesting techniques (1- vs. 2-way), and to elucidate the implications of such a sensitivity to model capability in reproducing meteorological and chemical observations.

2. Model description and evaluation methodologies

2.1. Model configurations and simulation design

The Houston–Galveston region in TX is a geographically-complex, highly-populated, and industrial-oriented region with more than 4 million people. The Gulf of Mexico provides warm, moist onshore flow on a daily basis. Large amounts of NO_x and volatile organic compounds (VOCs) are emitted from various sources including fossil-fuel refining plants, urban industry, oil refineries, transportation, and ship channels. High pollutant emissions, coupled with a warm, moist climate, make this region suffering from significant air pollution. The meteorology and chemistry in this area are extremely complex. The surface atmospheric conditions tend to be dominated by unstable conditions during daytime hours (7 a.m. to 5 p.m.) and very stable or stable conditions during nighttime hours (7 p.m. to 6 a.m.) (Fritz, 2003). Recent field and modeling studies have shown the impacts of large- and small-scale meteorological forcing on the formation and transportation of chemical species within this area (Daum et al., 2004; Banta et al., 2005; Bao et al., 2005; Jiang and Fast, 2004; Fast et al., 2006). The TexAQS 2000 represents a multi-organizational collaborative effort to study air quality and controlling factors in this area. Intensive ground-level meteorological and chemical observations were made at multiple sites throughout eastern TX. Aircraft measurements were also made by NOAA/NCAR Electra aircraft. Such data were sampled at a time resolution of 1-s for O_3, NO, and CO, and at 3-s for NO_2. In this study, a 5-day episode beginning 28 August 2000 at 12 Zulu (12Z) time through 2 September 2000 at 06Z over the eastern TX is selected for WRF/Chem model application and evaluation, because of O_3 non-attainment with maximum hourly-averaged O_3 mixing ratios at any of the sites of 112, 146, 199, 168, 124 and 125 ppb on 28 August–2 September, respectively. The 199 ppb O_3 on 30 August was the highest during the entire TexAQS 2000.

Two PBL schemes and three LSMs are examined in model simulations. The two PBL schemes are the Yonsei University (YSU) PBL scheme (Hong and Dudhia, 2003; Hong et al., 2006) and the Mellor–Yamada–Janjic (MYJ) scheme of Janjic (2002). The three LSMs are the National Center for Environmental Prediction, Oregon State University, Air Force, and Hydrologic Research Lab's (NOAH) LSM (Chen and Dudhia, 2001a, b; Ek et al., 2003), the simple thermal diffusion (Slab) scheme of Dudhia (1996), and the Rapid Update Cycle (RUC) LSM of Smirnova et al. (2000). The main difference between the two PBL schemes is that the YSU scheme is a non-local scheme that explicitly calculates turbulent kinetic energy (TKE) whereas the MYJ PBL scheme is a local 1.5 order TKE closure scheme. In local closure schemes, turbulent fluxes at various heights in the PBL are related to vertical gradients of mean variables at the same heights. Nonlocal closure works in the same way, but it estimates the fluxes at a certain point by analyzing the mean profiles over the entire domain of turbulent mixing, thus accounting for multiple-size eddies, making them more applicable to convective, unstable boundary layers (Bright and Mullen, 2002). By accounting for non-local mixing and the effect of large eddies by bulk properties of the PBL, YSU provides improved PBL treatment based on the Medium-Range Forecast (MRF) scheme (Hong and Pan, 1996). The PBL height is determined using a critical bulk Richardson number of 0. However, this may not be applicable for typical nighttime simulations, where the Richardson number is equal to zero at the surface. In this way, the PBL height is dependent only on the buoyancy profile. Entrainment at the PBL top is handled explicitly, rather than implicitly (Noh et al., 2003) and set proportional

to the surface buoyancy flux. The MYJ PBL scheme imposes a limit on the master scale over which mixing can occur, which is determined by TKE, buoyancy, and shear. This scheme determines the PBL height to be the lowest level at which TKE approaches its lower bound. The main differences among the three LSMs include the depths of soil and the land-surface processes treated. The slab LSM is a simple thermal diffusion scheme with 5 soil layers (1, 2, 4, 8, and 16 cm) built upon slight improvements to the force-restore method. It uses a 1-D equation to calculate surface heat fluxes and applies a linear soil temperature profile based on model parameters, though ideally it should be determined from the previous day's conditions (Dudhia, 1996). The NOAH LSM is a 4-layer (10, 30, 60, and 100 cm) soil model which incorporates canopy moisture, vegetation effects, runoff and drainage, and snow cover. Fluxes calculated within this scheme include sensible and latent heat fluxes to the PBL. Similar in physical complexity to the NOAH LSM, the RUC LSM treats one additional soil layer and also includes improved parameterizations for snow and frozen soil.

Table 1 summarizes various model configurations used for baseline and sensitivity simulations. The baseline simulation (i.e., N_Y or 1W12) is conducted using a pair of the NOAH LSM and the YSU PBL scheme at 12 km. The simulation code of 1W12 is used for the same baseline simulation to distinguish it from a sensitivity simulation at 12 km conducted concurrently with a nested 4-km simulation using 2-way nesting (i.e., 2W12) to facilitate discussions on model sensitivity to horizontal grid spacing and nesting methods. Three sensitivity simulations are conducted at 12 km to examine model sensitivity to different pairs of PBL schemes and LSMs: the slab/YSU pair (S_Y), the RUC/YSU pair (R_Y), and the NOAH/MYJ pair (N_M). In comparing results from different PBL schemes or LSMs, some differences may be attributed to other processes (e.g., radiation schemes) that are coupled with PBL schemes or LSMs and in turn affect their model performance. The impact of those coupled processes is, however, not examined in this study. Two simulations are conducted at 4 km to examine sensitivity to grid resolutions using 1-way (i.e., 1W4) and 2-way nesting (i.e., 2W4). Comparisons of 2W12 vs. baseline (i.e., 1W12) and 1W4 vs. 2W4 allow an examination of sensitivity to different nesting methods at different grid spacing. Fig. 1 shows the simulation domains at 12 and 4 km centered over the Houston–Galveston region in the eastern TX along with locations of 8 sites for detailed analyses.

All simulations use the Second Generation Regional Acid Deposition Model (RADM2) (Stockwell et al., 1990) and the Modal Aerosol Dynamics Model for Europe with Secondary Organic Aerosol Model (MADE/SORGAM) (Ackermann et al.,

Table 1
Model configurations used in WRF/Chem simulations [a].

a. Physical and chemical options

Physical and chemical processes	Scheme/setting for baseline simulations	Scheme/setting for sensitivity simulations
Shortwave radiation	Dudhia	The same as baseline
Longwave radiation	RRTM	The same as baseline
PBL process	YSU	MYJ
Land-surface process	NOAH	Slab, RUC
Cumulus	Kain-Fritsch	The same as baseline
Cloud microphysics	None	The same as baseline
Photolysis scheme	Madronich	The same as baseline
Gas-phase mechanism	RADM2	The same as baseline
Cloud chemistry	None	The same as baseline
Aerosol module	MADE/SORGAM	The same as baseline
Horizontal grid resolution	12 km	4 km
Nesting	None	1- and 2-way

b. Simulation types and codes

Simulation type	Simulation name	LSM	PBL scheme	Nesting
Baseline	N_Y [b]	NOAH	YSU	None
Sensitivity	S_Y	Slab	YSU	None
Sensitivity	R_Y	RUC	YSU	None
Sensitivity	N_M	NOAH	MYJ	None
Baseline	1W12 [b, c]	NOAH	YSU	None
Sensitivity	1W4 [c]	NOAH	YSU	1-way
Sensitivity	2W12 [c]	NOAH	YSU	2-way
Sensitivity	2W4 [c]	NOAH	YSU	2-way

[a] Acronyms: RRTM — Rapid Radiative Transfer Model; YSU — Yonsei University; MYJ — Mellor–Yamada–Janjic; NOAH — National Center for Environmental Prediction, Oregon State University, Air Force, National Weather Service's Hydrologic Research Lab; RUC — Rapid Update Cycle; RADM2 — Second Generation Regional Acid Deposition Model; MADE/SORGAM — Modal Aerosol Dynamics Model for Europe with Secondary Organic Aerosol Model; LSM — land-surface model; PBL — planetary boundary layer; N_Y — NOAH/YSU pair; S_Y — slab/YSU pair; R_Y — RUC/YSU pair; N_M — NOAH/MYJ pair; 1W12 — no nesting at 12 km; 1W4 — one-way nesting at 4 km; 2W12 — two-way nesting at 12 km; and 2W4 — two-way nesting at 4 km.

[b] The simulations N_Y and 1W12 refer to the same baseline simulation conducted with NOAH/YSU pair at a horizontal grid spacing of 12 km without nesting. The results from this baseline simulation are used to provide initial and boundary conditions to nested 4-km simulation (i.e., 1W4) using one-way nesting. The code "1W12" is given to distinguish it from a concurrent simulation at a 12-km grid resolution and a nested 4-km grid resolution (i.e., 2W12) in discussing model results with different nesting methods.

[c] 1W12 and 1W4 are conducted sequentially using 1-way nesting in two model simulations, whereas 2W12 and 2W4 are conducted concurrently using 2-way nesting in one model simulation.

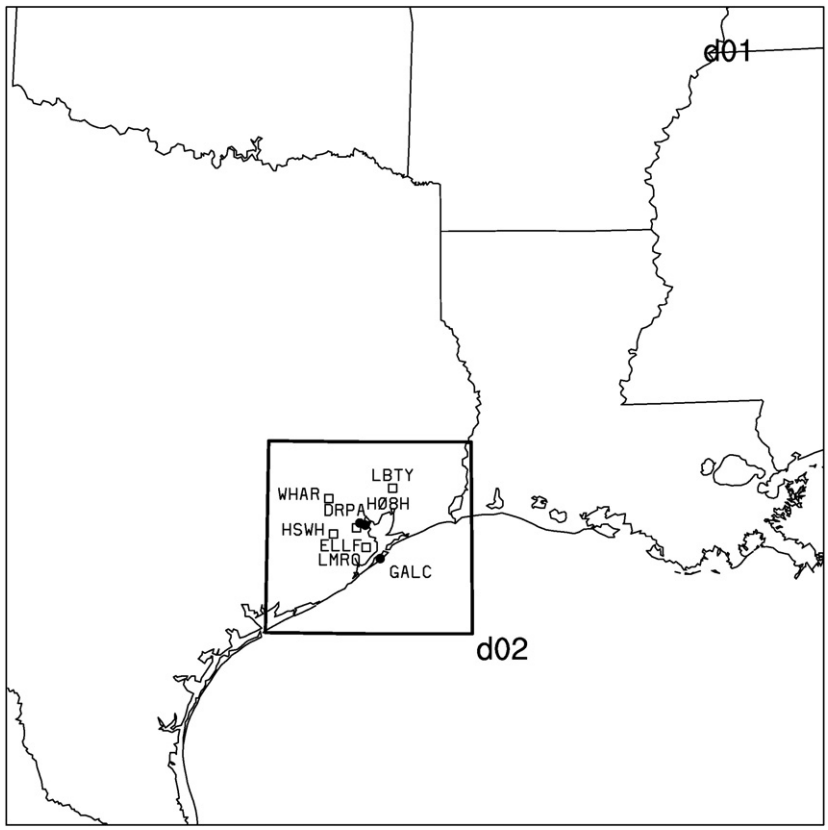

Fig. 1. The modeling domains at 12-km (d01) and 4-km (d02) over eastern Texas. Detailed analyses of meteorological and chemical predictions are conducted at three sites (in black dot): Dear Park (DRPA), Galveston Airport (GALC), and LaPorte (H08H). Additional evaluation is conducted for PBL height predictions using available radar wind profilers measurements at five sites around Houston (in hollow square): Wharton (WHAR), Ellington Field (ELLF), Southwest Houston (HSWH), Liberty (LBTY), and LaMarque (LMRQ).

1998; Schell et al., 2001). A 60-s time step is used for online-coupled simulations. The model inputs are based on Fast et al. (2006) who conducted WRF/Chem simulations over the same domain using the Carbon Bond Mechanism version Z (CBM-Z) and the Model for Simulating Aerosol Interactions and Chemistry (MOSAIC). Emissions for RADM2 and MADE/SORGAM at 12 km and those for CBM-Z and MOSAIC at 12 and 4 km are provided by Pacific Northwest National Laboratory (PNNL) (Jerome Fast, PNNL, personal communications, 2004). In this study, the 4-km emissions for CBM-Z and MOSAIC of Fast et al. (2006) are mapped to RADM2 and MADE/SORGAM, based on gas-phase species mapping provided by PNNL (Rahul Zaveri, PNNL personal communication, 2006) and aerosol species mapping through comparing the MOSAIC and MADE/SORGAM 12-km emissions. The 24-category U.S. Geological Survey (USGS) land use and land cover dataset are used for all simulations and they are interpolated by the WRF Preprocessor System (WPS) to 4 and 12 km. Meteorological initial and boundary conditions (ICONs and BCONs) are derived from the North American Regional Reanalysis (NARR) (http://www.emc.ncep.noaa.gov/mmb/rreanl/). Chemical ICONs and BCONs are horizontally homogeneous. Emissions inventories are taken from the Texas Commission on Environmental Quality (TCEQ) for gases and from the EPA's National Emissions Inventory 1999 version 3 (NEI-99 v. 3) for PM species. A built-in program in WRF/Chem is used to create ICONs and BCONs at 4 km (i.e., 1W4) from the 12-km baseline outputs (i.e., 1W12).

2.2. Evaluation protocols

Model evaluation is conducted in terms of temporal variation and spatial distribution at surface, vertical profiles, and domain-wide performance statistics. Statistical parameters include correlation coefficient (corr), mean bias (MB), mean absolute gross error (MAGE), root mean-square error (RMSE), normalized mean bias (NMB), and normalized mean error (NME), as described in Zhang et al. (2006a). Simulated vertical profiles of chemical species are compared with aircraft measurements taken by three flights during the simulation period. Unlike a sonde, the aircraft moved quickly in the horizontal direction relative to the vertical direction. In-situ measurements of species concentrations were obtained during takeoff and in flight at different heights; they may not be directly compared to grid-volume averages of the model concentration predictions. A rough comparison may be conducted, however, using measurements taken during aircraft takeoff with its fast upward movement, resulting in a vertical profile that can be used to evaluate simulated vertical profiles. An approximate approach is developed in this study to conduct such a rough comparison, assuming that the measured vertical profile during the

aircraft take-off trajectories is similar to an atmospheric sounding profile. In this approach, latitude and longitude data are averaged to find the average position of the aircraft during the flight time. Using this information, the corresponding grid cell can be found and the simulated vertical profiles of meteorological variables and chemical species from that cell are used to compare with the vertical measurements made by the aircraft. Although a similar approach has been used in other studies (e.g., Zhang and Han, 2007), this approach has several limitations. For example, the aircraft observations and model simulations are not on the exactly same time scale and at the exactly same latitude and longitude. Also, mobile measurements are compared with a point-specific location using an approximate averaging method that involves certain assumptions.

3. Model evaluation and sensitivity analysis

3.1. Model performance and sensitivity to PBL schemes and LSMs

3.1.1. Meteorological predictions

3.1.1.1. Spatial distributions and domain-wide performance statistics. Fig. 2 shows the spatial distributions of temperature (T2) and relative humidity (RH2) at 2 m and PBL height (PBLH) from simulations N_Y, S_Y, N_M, and R_Y at 20 UTC (3PM CDT) on 30 August 2000. The overall performance statistics for major meteorological variables (i.e., T2, RH2, wind speeds and direction at 10 m (WS10 and WD10), *U* and *V* components of wind speeds (U10 and V10), and PBLH) are summarized in Table 2. YSU and MYJ PBL schemes give similar T2 predictions over most of the domain, with slightly lower T2 by MYJ along the coastline and over the Gulf of Mexico, due to differences in temperature advection under the influence of coastal fronts and land–sea breezes simulated by the two schemes. Larger sensitivity is found among simulations with different LSMs, driven by differences in their predictions of latent heat fluxes and surface sensible heat fluxes. Among the three LSMs, Slab gives the lowest T2, RUC gives the highest T2 over most of the domain. Domain-wide performance statistics against available T2 observations at 32 sites indicate the largest cold bias (−1.3 °C) by S_Y and the smallest one (−0.1 °C) by R_Y. NOAH and RUC include more complex formulations and deeper soil layers (100 cm and 300 cm, respectively) than Slab that has a simple formulation for dynamics of soil moisture and a shallow soil depth of 16 cm, therefore capturing observed T2 better in terms of both the magnitude and spatial variability. The MYJ PBL scheme gives slightly higher (5–10%) RH2s than YSU. Similar to T2, the model shows a larger sensitivity in RH2 predictions to LSMs. Slab gives higher moistures than NOAH or RUC, due to higher latent heat fluxes and lower surface sensible heat fluxes (figure not shown), which has large effects on T2 and PBLH, as indicated by Chen and Dudhia (2001b). Interestingly, Slab gives the lowest MB and NMB (1.5% and 2.5%, respectively) in RH2 among the four runs, likely resulted from the large cold bias in T2 predictions that may lead to higher RH2. Other simulations give moderate negative MBs and NMBs. Spatial distributions of wind fields simulated by YSU and MYJ and by the three LSMs are similar (figures not shown). Among all simulations, S_Y gives the lowest MB (~0.05 m s^{-1}) in WS10, with moderate MBs (0.4–0.8 m s^{-1}) for other simulations. One caveat in calculating statistics for wind direction is treating this vector as a scalar (Zhang et al., 2006a). For example, wind directions of 350° (NNW) and 10° (NNE) are actually only 20° apart on a wind rose plot. Numerically, the difference between the two is 340°, which may result in misleading statistics. Using MB to determine the model's performance may be misleading when the differences between observed and simulated WD are greater than 180°. Performance statistics are therefore calculated for U10 and V10, in addition to WD10. Slab gives the smallest MB in U10 and V10, but the largest bias in WD10 among the four simulations. Although the domain-wide MBs are much smaller than 180° for all simulations, the situation with the misleading MBs may occur at individual sites or during some hours, thus affecting the overall accuracy of the statistics for WD. Different from WS10, the domain-wide statistics for WD10 by the four simulations are fairly similar (NMBs of 5.7–7.5%). Compared with PBLH from N_Y, N_M gives overall lower values (by up to 500–2000 m) throughout the domain, particularly over western Mississippi and along the coastline (where the terrain is complex), which are in better agreement with observations (NMBs are 22.7% vs. 54.4%). PBLH predictions are sensitive to LSMs. S_Y shows much lower (1000–1500 m) values than N_Y and R_Y. All four simulations overpredict (NMBs of 22.7–54.4%) PBLHs with lower biases by N_M and S_Y. Among all variables examined, the largest differences between the two PBL schemes are found in PBLHs, consistent with Mao et al. (2006).

3.1.1.2. Temporal variations. Fig. 3 shows time series plots for T2, RH2, WS10, and WD10 at two sites: Deer Park (DRPA) and Galveston Airport (GALC), TX. DRPA and GALC are located about 20 and 50 miles, respectively, from downtown Houston, TX. GALC is affected by bay/sea breezes because of its proximity to the coast of Gulf of Mexico. The largest emissions of primary pollutants such as VOCs occur along the ship channel between downtown Houston and Galveston Bay. Therefore, an accurate portrayal of these meteorological patterns is needed to identify areas inundated with O_3 precursor emissions. Observed T2 values are well reproduced at DRPA in terms of maximum, minimum, and diurnal variations by all four simulations except S_Y with the Slab LSM on days 4 and 5 when S_Y exhibits the largest cold bias during daytime and nighttime (consistent with T2 statistics in Table 2). Compared with DRPA, the strong land–sea interactions at GALC result in a smaller variation in observed T2 during daytime and at night. None of the four simulations reproduce T2 at GALC, with much weaker diurnal variations and smaller daytime maxima than observations as well as little sensitivity to either PBL schemes or LSMs. This is likely because of model difficulties in capturing small-scale meteorology in areas affected by sea/bay breezes. Deviations between simulated and observed T2 appear to grow with time during days 3–5 at DRPA, due to the lack of a data assimilation system in this version of WRF/Chem. Large deviations exist between observed and simulated RH2 as well as among the four simulations. While N_Y and N_M give similar underpredictions on days 3–5 at DRPA and GALC,

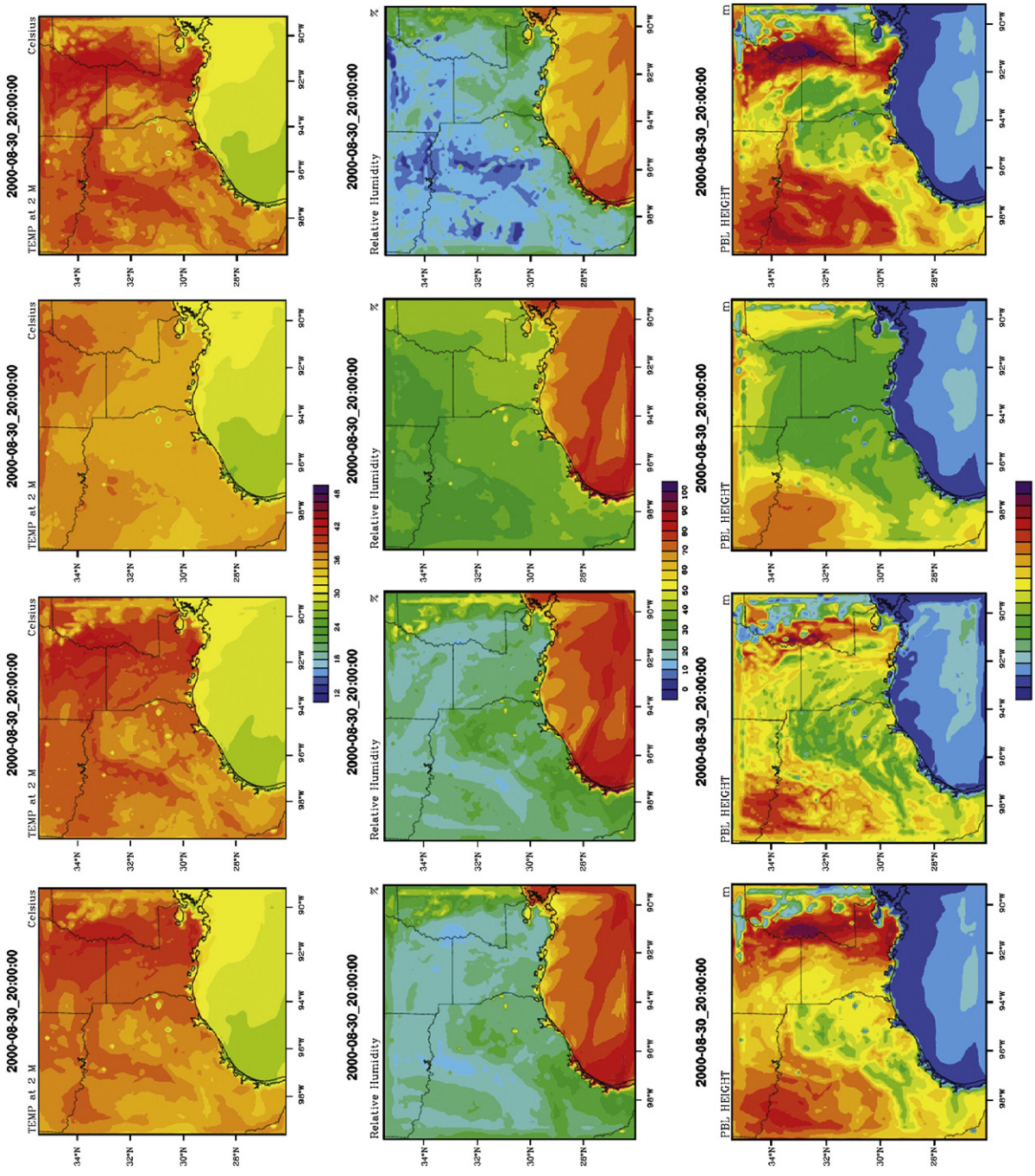

Fig. 2. Spatial distributions of temperature (T2) and relative humidity (RH2) at 2 m and PBL height (PBLH) from simulations (left to right) N_Y, N_M, S_Y, and R_Y at 20 UTC (3PM CDT) on 30 August 2000.

Table 2
Normalized mean biases (NMBs) of meteorological variables for all simulations.

	T2, °C		RH2, %		WS10		WD10, deg		U10, m s^{-1}		V10, m s^{-1}		PBLH, m	
	MB	NMB,%	MB	NMB,%	MB	NMB,%	MB	NMB,%	MB	NMB,%	MB	NMB,%	MB	NMB,%
N_Y (1W12)	−0.7	−0.3	−17.2	−27.4	0.4	12.6	13.8	6.6	0.4	21.6	−0.8	−34.6	592.3	54.4
N_M	−0.4	−1.2	−13.5	−21.7	0.8	27.1	13.4	6.4	−0.4	−18.4	−0.6	−28.1	247.3	22.7
S_Y	−1.3	−4.1	1.5	2.5	0.0	1.7	15.7	7.5	−0.2	−11.7	−0.3	−14.4	264.2	24.3
R_Y	−0.1	−0.3	−19.7	−30.5	0.7	24.2	12.0	5.7	0.5	25.4	−0.5	−23.0	584.5	53.7
1W4	−2.3	−7.4	−6.2	−9.3	−0.1	−4.8	26.5	12.1	0.3	13.0	−0.7	−33.0	−29.5	−2.7
2W12	−0.6	−1.8	−12.3	−18.4	0.7	22.8	23.2	10.6	0.2	13.0	−0.8	−37.0	643.4	59.3
2W4	−0.9	−2.8	−14.4	−21.6	0.2	6.4	28.7	13.1	0.3	16.0	−0.7	−31.0	586.4	53.8

N_Y — NOAH/YSU pair; N_M — NOAH/MYJ pair; S_Y — slab/YSU pair; R_Y — RUC/YSU pair; 1W12 — one-way 12 km, which is the same as N_Y; 1W4 — one-way 4 km; 2W12 — two-way 12 km; and 2W4 — two-way 4 km. T2 — temperature at 2 m; RH2 — relative humidity at 2 m; WS10 — wind speed at 10 m; WD10 — wind direction at 10 m; U10 — *U* component of WS10; V10 — *V* component of WS10; and PBLH — planetary boundary layer height.

larger differences are found among N_Y, S_Y, and R_Y with different LSMs, indicating a higher sensitivity of RH2 predictions to LSMs. While S_Y overpredicts RH2 on days 3–5, N_Y and R_Y both significantly underpredict RH2 with lower values by R_Y at DRPA. At GALC, all simulations underpredict RH2, particularly on days 3–5.

Simulated wind speeds are sensitive to both PBL schemes and LSMs in terms of their temporal variations and magnitudes, with large differences between N_Y and N_M on some days (e.g., days 1, 2, and 5 at DRPA and days 1 and 3–5 at GALC) and among N_Y, S_Y, and R_Y on days 3–5 at both locations. At both sites, N_Y performs reasonably well and S_Y shows a negative nighttime bias, particularly at GALC. Compared with N_Y, N_M gives higher WS10 during daytime but lower values during most nighttime at DRPA and either higher or lower values throughout the 5-day period at GALC. R_Y gives higher WS10 than either N_Y or S_Y at DRPA and either higher or lower values at GALC. However, diurnal

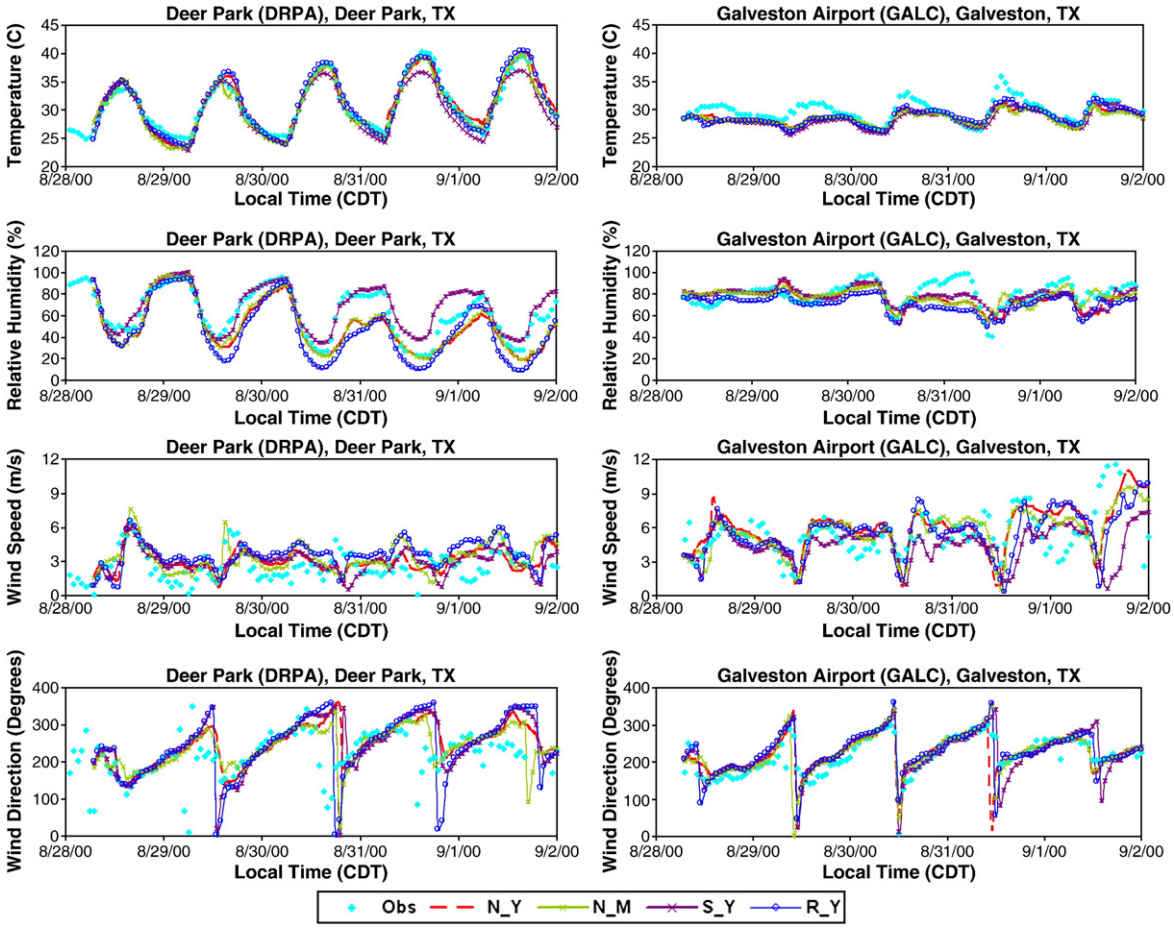

Fig. 3. Observed and simulated time series of temperature (T2) and relative humidity (RH2) at 2 m, wind speed (WS10) and direction (WD10) at 10 m from simulations N_Y, N_M, S_Y, and R_Y at Deer Park (DRPA) and Galveston Airport (GALC), TX.

variations among the four simulations are similar. The observed wind fields at GALC are dominated by an onshore flow on 28–29 August, and a shore-parallel or offshore large-scale flow and the stagnant or near-stagnant conditions during noontime (~12:00 CDT) on the remaining days. The change of the wind direction from north-westerlies in the morning to southerlies or south-easterlies in the afternoon and the stagnant flow provide good indications of the impact of the land–sea breeze at GALC, particularly on 30–31 August. The north-westerlies in the morning carry the pollutants from the Houston area to GALC, the near-stagnant condition during noontime helps the pollutants to accumulate at GALC, resulting in the highest $PM_{2.5}$ concentrations that typically occur 1 or 2 h lag behind the stagnant wind condition (see Fig. 7). The observed WD10 shifts are generally reproduced at GALC. Compared with observations, larger biases exist in WD10 predictions at DRPA than at GALC. In general, large discrepancies between observed and simulated values occur during late afternoon into evening hours at both locations for all 5 days. For WD10 predictions, large sensitivity is found at DRPA between N_Y and N_M and among N_Y, S_Y, and R_Y, with the largest deviation occurring at DRPA in R_Y on days 3–5 when wind direction shifts in late afternoon. Although the magnitude of observed WD10 shift is not well represented by R_Y, R_Y actually simulates the WD10 shifts more accurately in time.

During the TeXAQS2000, radar wind profilers were deployed at five locations around Houston (i.e., Wharton (WHAR), Ellington Field (ELLF), Southwest Houston (HSWH), Liberty (LBTY), and LaMarque (LMRQ)) to measure PBLH at hourly intervals up to 3 km above ground level (AGL). Those data are used to evaluate simulated PBLHs as shown in Fig. 4. Compared with observations, all four simulations give deeper PBLHs for most times at all the sites. The daytime development and growth of the PBL are generally well represented, although initial growth appears to be too fast, particularly on day 1. Simulated heights at LBTY and LMRQ appear to be significantly overpredicted on days 3–5 as compared with other locations. Sites DRPA and ELLF are nearly co-located with 5 miles apart, allowing an approximate comparison between PBLH and RH. There seems to be some correlations with the underprediction of RH and the overprediction of PBLH. For example, on day 5, RH values at DRPA are underestimated by 36.4% from N_Y and PBLH values at ELLF are overestimated by 51.8% (1022.4 m). Higher surface heat fluxes from N_Y could lead to decreased RH and higher PBLH. Compared with N_Y, N_M generally simulates a more accurate representation of PBLHs in terms of both magnitudes and temporal variations (with NMBs of 22.7% vs. 54.4% for N_M and N_Y, respectively). Overall, N_M gives lower PBLHs during daytime but higher PBLHs during nighttime than N_Y, except daytime during day 5 at WHAR. The assumptions and parameters used in the two PBL schemes may help explain these differences. For example, the YSU scheme arbitrarily sets an unrealistic value of 15 m for nocturnal PBLH, leading to lower PBLHs than N_M at night. This problem has been corrected in WRF/Chem v. 3.0 (Hong et al., 2008). On the other hand, N_M simulates nighttime values on the order of hundreds of meters, which is more consistent with meteorological dynamics and also allows better capture of nighttime species concentrations. Among the three simulations with different LSMs, S_Y appears to simulate PBLHs that more closely

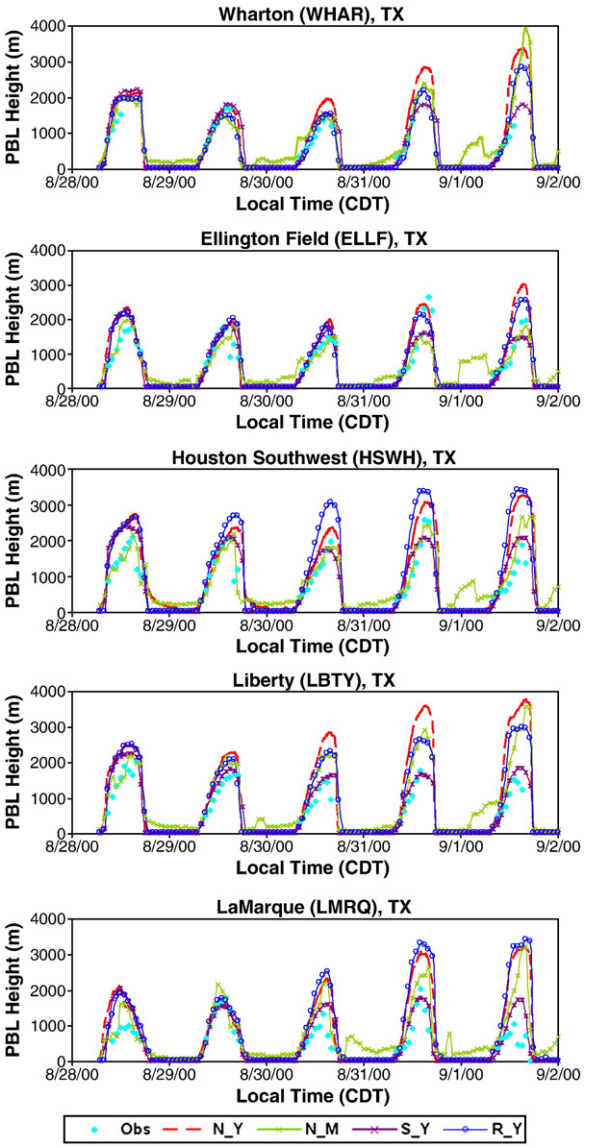

Fig. 4. Observed and simulated time series of PBL heights from simulations N_Y, N_M, S_Y, and R_Y at Wharton (WHAR), Ellington Field (ELLF), Houston Southwest (HSWH), Liberty (LBTY) and LaMarque (LMRQ), TX.

correspond to observations. Discrepancies among simulated PBLHs can be explained by differences in surface sensible heat fluxes simulated by each LSM. For example, at HSWH on 30 August, R_Y and N_Y give the highest and the second highest surface sensible heat fluxes. Consequently, their simulated PBLHs are also the highest and the second highest, respectively. At LMRQ on 30 August, surface sensible heat fluxes simulated by N_Y, N_M, and R_Y are similar, all of them give much higher values than S_Y, leading to similar PBLHs by N_Y, N_M, and R_Y but much lower PBLHs by S_Y. Compared with N_Y and R_Y, the more accurate PBLHs by S_Y may be attributed to lower sensible heat fluxes from the surface (resulted from the cold bias in T2 in S_Y, see Fig. 2 and Table 2). For comparison, higher sensible heat fluxes in N_Y and R_Y may lead to higher T2, lower RHs, and higher simulated PBLHs.

3.1.1.3. Vertical profiles. Vertical profiles of simulated temperature (T) and relative humidity (RH) are compared with measurements taken from the NOAA's Electra aircraft during takeoff in Fig. 5. Three flights were made during 15 UTC (10 a.m. CDT) 28 August, 17 UTC (12 p.m. CDT) 30 August, and 17 UTC (12 p.m. CDT) 1 September 2000. The simulated vertical T distributions correspond relatively well with observations on 28 August but deviate more significantly below 1500 m on other days. The observed stable layers between 486 and 600 m on 30 August and between 532 and 779 m on 1 September are not well captured by all simulations, although S_Y and N_M give a thin stable layer (less than 184 and 87 m, respectively) on 30 August at a much higher altitude than observed. N_Y, N_M, and R_Y perform similarly, whereas S_Y gives lower T at the surface and in the PBL.

Compared with T profiles, larger differences occur among RH profiles. Although N_Y either significantly underpredicts (28 August and 1 September for most heights) or significantly overpredicts (30 August at an altitude of 500 m or higher), variation trends in RH with height for some heights (e.g., decrease with increasing height between ~1000 m and ~2500 m on August 28 and increase with increasing height between ~1500 m and ~3500 m on August 30 and between ~700 m and ~2500 m on September 1) are generally

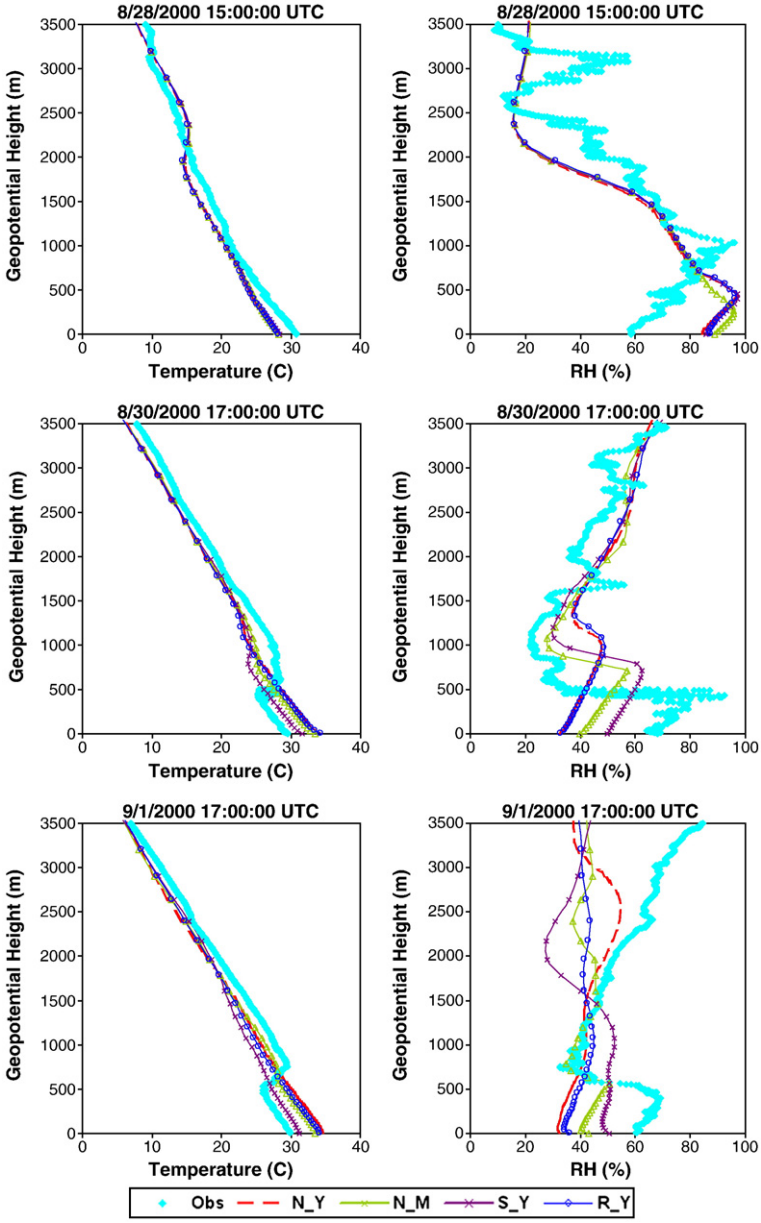

Fig. 5. Observed and simulated vertical profiles of temperature (T) and relative humidity (RH) from simulations N_Y, N_M, S_Y, and R_Y. Observational data are taken from the NOAA's Electra aircraft instrumentation during three flight takeoffs at 15 UTC, August 28, 17 UTC August 30, and 17 UTC September 1, 2000.

captured by N_Y with deviations in RH of 0 to ±25%. N_M also captures well the vertical variability in RH with height. It simulates lower level (<1500 m) RHs more accurately than N_Y on 30 August and 1 September. At altitudes between 1500 and 3000 m on 1 September, N_Y generally gives closer agreement with observations. While R_Y gives similar RH profiles to N_Y, larger differences occur in simulated RH profiles by S_Y. Different LSMs may give opposite RH variation trends. For example, S_Y simulates decreasing RH from 1000 to 2000 m while N_Y, R_Y, and observations all show increasing RH with height on 1 September.

3.1.2. Chemical predictions

3.1.2.1. Spatial distributions. All four simulations are able to simulate high CO, O_3, and $PM_{2.5}$ in and downwind of major metropolitan areas (e.g., Houston, Dallas, San Antonio, and New Orleans). Offshore flow appears to be most evident on days 2–4, as extremely high O_3 occur over the Gulf of Mexico. Fig. 6 shows the spatial distributions of CO, O_3, and $PM_{2.5}$ from N_Y, N_M, S_Y, and R_Y at 20 UTC (3PM CDT) on 30 August 2000. Among the four simulations, S_Y gives the highest CO mixing ratios over most of the domain. Although S_Y gives the largest cold bias in T2, it also gives the shallowest PBL (see Fig. 2); the latter effect dominates, resulting in the highest simulated concentrations for slow-reacting pollutants such as CO. Similarly, N_M gives lower PBLHs than N_Y and R_Y, leading to the second highest CO concentrations. N_Y gives the highest PBLHs among the four simulations, resulting in the lowest CO concentrations over the entire domain. These results are fairly consistent with the domain-wide statistics for CO shown in Table 3, with NMBs of −37.3%, −24.1%, −14.9%, and −33.2% for N_Y, N_M, S_Y, and R_Y, respectively. O_3 is a secondary pollutant and $PM_{2.5}$ consists of secondary components. Their concentrations and spatial distributions are affected not only by meteorology (e.g., T2 and PBLH) but also emissions of their precursors and the resulting tropospheric oxidizing capacities. The effects of latter factors may be nonlinear. For example, higher T values can lead to higher tropospheric oxidizing capacities thus higher O_3 formation, whereas higher PBL heights can reduce O_3 level through ventilation of high emissions and concentrations. Lower T and higher RH values can lead to higher $PM_{2.5}$ formation through increasing the concentrations of volatile PM species such as nitrate and secondary organic aerosol, they may also decrease the formation of non-volatile and photochemically-dependent PM species such as SO_4^{2-}. As a consequence of these competitions between meteorological and chemical effects, N_M gives the highest O_3 mixing ratios, S_Y gives the highest $PM_{2.5}$ concentrations, and N_Y gives the lowest O_3 mixing ratios and $PM_{2.5}$ concentrations domain-wide at 3 p.m. CDT 30 August. Although S_Y gives the coldest T2 that is not favorable to the photochemical formation of O_3, it gives the lowest PBLH and therefore the highest mixing ratios for its precursors, leading to relatively higher O_3 than N_Y and R_Y that have higher T2 but also higher PBLH. These results are somewhat inconsistent with statistics shown in Table 3, because of the inclusion of all hourly O_3 and $PM_{2.5}$ concentrations (rather than values at 3 p.m. CDT) for statistics calculations and the fact that larger biases occur in nighttime O_3 mixing ratios for all simulations and in nighttime $PM_{2.5}$ concentrations for N_Y and R_Y. While S_Y gives the least domain-wide O_3 overpredictions (with an NMB of 9.7%), it gives the highest bias in $PM_{2.5}$ predictions (with an NMB of 14.6%). N_Y gives the largest domain-wide O_3 overpredictions (with an NMB of 26.1%) but its NMB for $PM_{2.5}$ is the second smallest (−1%). Compared with an NMB of 27.9% in nighttime O_3 mixing ratios in N_Y that simulates nighttime PBL relatively well, the domain-wide O_3 biases in N_Y, S_Y, and R_Y are dominated by nighttime high biases (NMBs of 83.1%, 33.2%, and 46.7%, respectively). The seemingly low NMB in nighttime O_3 mixing ratios in S_Y is due to much higher nighttime NO_2 mixing ratios (with MB and NMB of 28 ppb and 190%) that titrate more O_3 to form NO_3 radicals at night. Although the domain-wide biases in NO_2 are high for all four simulations (NMBs of 54.9–110%), they are dominated by nighttime large biases that have relatively small impacts on domain-wide O_3 performance. Several factors contribute to the high biases in NO_2 in all simulations. For example, uncertainties may exist in NO_x emissions based on the EPA NEI99 version 3. The quasi steady state approximation (QSSA) is used to solve nitrogen chemistry, in particular, diagnose NO in the RADM2 gas-phase mechanism implemented in WRF/Chem. QSSA may not be valid for this particular episode, which leads to high NO_x and NO_y at night. For simulations using the YSU scheme, the poor representation of nocturnal PBL further worsens nighttime overpredictions. Similarly, NMBs for NO mixing ratios are also high, ranging from −80.2% to −74.7%.

3.1.2.2. Temporal variations. Fig. 7 simulates observed and simulated hourly concentrations of CO, NO, NO_2, O_3, and $PM_{2.5}$ at DRPA, TX and those of NO, NO_2, O_3, and $PM_{2.5}$ at GALC, TX. Since no CO measurements are available at GALC, observed CO mixing ratios at LaPorte are shown in Fig. 7. LaPorte is about 25 miles from downtown Houston, TX, about 8 miles southeast of DRPA, and about 35 miles northwest of GALC. It is a coastal site that is strongly affected by bay breezes. Compared with observations, all simulations give much lower CO during daytime but much higher values at night at DRPA. At LaPorte, all simulations overestimate CO mixing ratios for most times. At several sites (figure not shown), the underpredictions override the overpredictions, leading to a domain-wide underestimation as shown in Table 3. Among the four simulations, N_Y performs the best for CO in terms of temporal variations and magnitudes at both sites, although the worst in terms of domain-wide statistics. The underestimations during the daytime are most likely related to the overestimation in PBLHs, which provides a greater effective mixing volume for species to dilute. On average during periods of higher simulated CO mixing ratios, values simulated by N_M are typically 70–900 ppb higher than those simulated by N_Y. Among three simulations with different LSMs, S_Y gives the highest CO, due to the lowest simulated PBLHs as shown in Figs. 2 and 4.

The largest differences among these simulations (in particular between S_Y and other simulations) are found in the mixing ratios of CO, NO_2, and $PM_{2.5}$ on August 31 at DRPA and in those of O_3 on September 1–2 at GALC. This is because of the largest differences in simulated meteorological variables (some are shown in Fig. 3). For example, S_Y gives the lowest T and PBLH and highest RH on August 31 at DRPA, leading to the highest concentrations of CO, NO_2, and $PM_{2.5}$. S_Y gives the lowest PBLH on September 1–2 at GALC, which

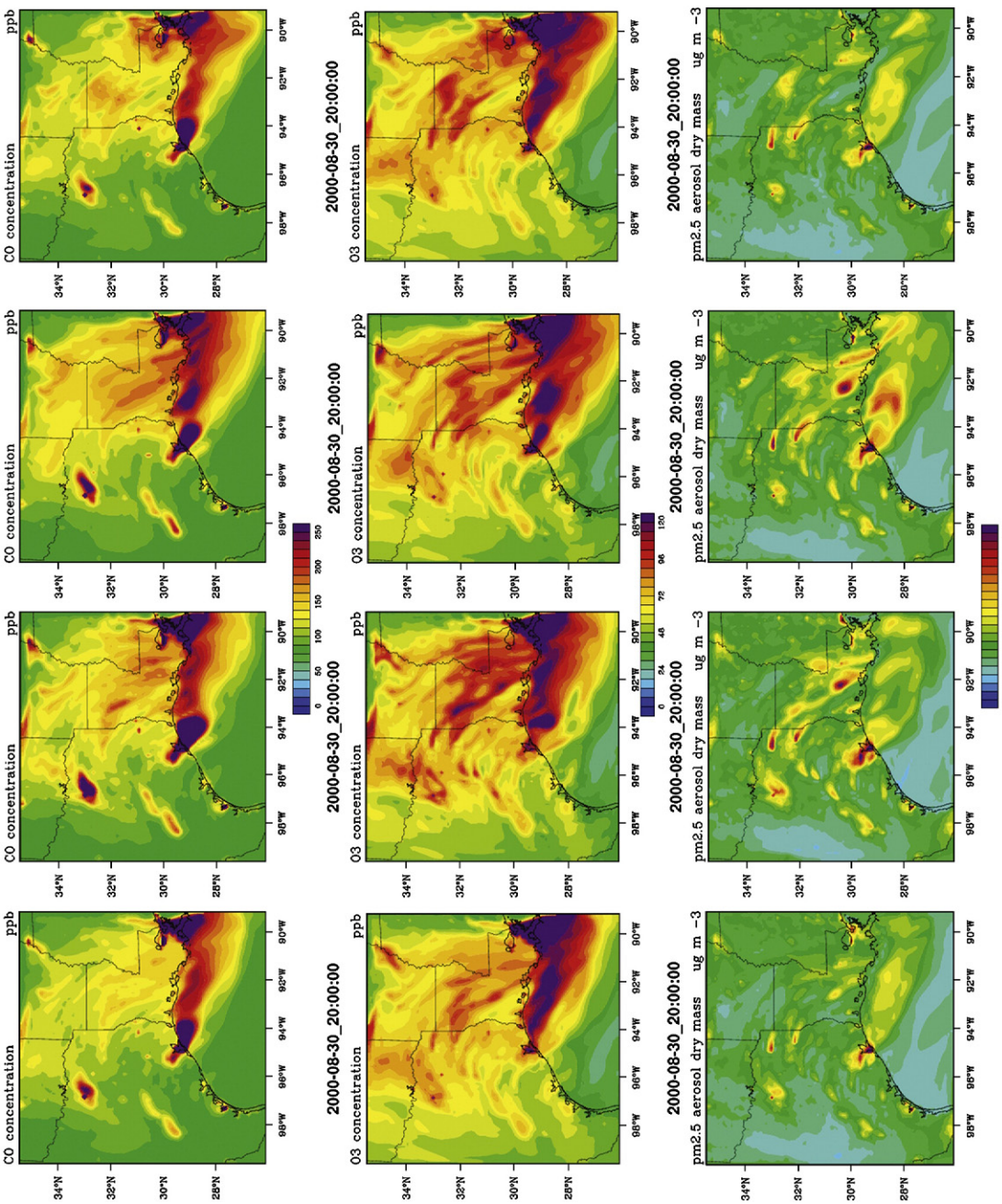

Fig. 6. Spatial distributions of CO, O_3, and $PM_{2.5}$ from simulations N_Y, N_M, S_Y, and R_Y at 20 UTC (3PM CDT) on 30 August 2000.

Table 3
Normalized mean biases (NMBs) of chemical concentrations for all simulations.

	O_3, ppb		NO, ppb		NO_2, ppb		CO, ppb		$PM_{2.5}$, μg m^{-3}	
	MB	NMB,%	MB	NMB,%	MB	NMB,%	MB	NMB,%	MB	NMB,%
N_Y (1W12)	10.2	26.1	−6.0	−80.2	7.3	54.9	−158.1	−37.3	−0.1	−1.0
N_M	4.1	10.5	−5.7	−75.9	11.0	83.2	−102.2	−24.1	−0.6	6.1
S_Y	3.8	9.7	−5.6	−74.7	14.5	110.0	−63.4	−14.9	1.47	14.6
R_Y	5.3	13.4	−5.7	−76.4	7.9	60.4	−140.6	−33.2	−0.1	−0.5
1W4	7.4	19.1	−4.4	−59.2	32.1	242.0	253.0	65.0	−2.6	−22.3
2W12	11.0	27.7	−6.0	−79.8	13.3	100.0	−127.1	−33.0	−4.1	−32.8
2W4	10.5	25.8	−5.3	−71.0	20.4	154.0	222.2	140.0	−4.3	−35.1

N_Y — NOAH/YSU pair; N_M — NOAH/MYJ pair; S_Y — slab/YSU pair; R_Y — RUC/YSU pair; 1W12 — one-way 12 km, which is the same as N_Y; 1W4 — one-way 4 km; 2W12 — two-way 12 km; and 2W4 — two-way 4 km.

leads to the highest concentrations of CO, NO, NO_2, O_3, and $PM_{2.5}$.

The four simulations perform similarly in terms of NO, although S_Y simulates slightly higher mixing ratios at both sites. Contrastingly, significant differences among model simulations occur for NO_2. S_Y simulates much higher (up to 60 ppb) mixing ratios of NO_2 at DRPA for most times than other simulations. While all four simulations generally reproduce the temporal variability of O_3, overpredictions occur at both sites for most times. None of the four simulations, however, are able to reproduce the peak O_3 values on days 3–4 at DRPA when the highest maximum hourly average O_3 values were recorded at many sites including DRPA for the TexAQS-2000. This may be attributed to several factors including inaccurate meteorological predictions such as sea/bay breezes that cause elevated pollutant levels in the mid-afternoon, underestimations in emissions of light olefins (e.g., ethane, propene) (Wert et al., 2003; Jiang and Fast, 2004), and the use of a typical mean emission variation profile (instead of an episodic profile that is more realistic). NOAA aircraft detected an emission event with a plume of very high olefin (>100 ppb) emitted from around 2.5 km north of DRPA at ~10:40 a.m. on 30 August that may have caused high O_3 mixing ratios observed at DRPA and LaPorte. Such episodic emissions are not represented in the emissions used here, leading to a failure of capturing the observed peak O_3 mixing ratios at DRPA. At DRPA, N_M and S_Y capture nighttime O_3 better than R_Y and N_Y. At GALC, all four simulations significantly overestimate daytime O_3 on all days except day 3, indicating difficulties in simulating O_3 over areas with land/sea coverage at a small temporal scale. Among the four simulations, N_M gives the most accurate nighttime O_3 mixing ratios, due mainly to the best representation of nocturnal PBL. S_Y gives low nighttime O_3 values, due to large simulated mixing ratios of NO_x that lead to significant titrations of O_3.

$PM_{2.5}$ concentrations are overall well reproduced at GALC (except the peak $PM_{2.5}$ values on 31 August and 1 September) but significantly overpredicted (by 37% to a factor of 12) for nearly all times at DRPA by all four simulations. Possible reasons for the large overestimations at DRPA include uncertainties in emission estimates of primary $PM_{2.5}$ species (such as black carbon (BC) and organic matters (OMs)), insufficient dry deposition, as well as a high initial $PM_{2.5}$ concentration of 8 μg m^{-3} used throughout the domain. Observed $PM_{2.5}$ composition is only available at one site at surface (i.e., LaPorte) and one site aloft (Williams Tower). The comparison of observed and simulated $PM_{2.5}$ composition at LaPorte shows large overpredictions for BC and OM which might be the case throughout the domain. N_M gives slightly higher $PM_{2.5}$ than N_Y at both sites for most times. Larger discrepancies exist among three simulations with different LSMs. Similar to CO and NO_2 predictions, S_Y generally gives the highest $PM_{2.5}$ among the four simulations (higher by 13 to 16 μg m^{-3} on average), due mainly to the lowest PBLHs during daytime and an unrealistically low nocturnal PBL prescribed in the YSU PBL schemes.

3.1.2.3. Vertical profiles. Fig. 8 shows observed and simulated vertical profiles of CO, NO, NO_2, and O_3 during three flight takeoffs at 15 UTC, 28 August, 17 UTC, 30 August, and 17 UTC, 1 September, 2000 from the four simulations. While all four simulations reproduce vertical profile of CO on 28 August and the vertical variation trends on 30 August and 1 September, large deviations exist in terms of magnitudes on 30 August and 1 September. Compared with N_Y, CO mixing ratios simulated by N_M decrease less rapidly with height in the lower layers. S_Y also simulates a slower decrease in CO mixing ratios with height than N_Y and R_Y, with the highest surface concentrations among the four simulations. It is interesting to note that the vertical profiles simulated by N_M and R_Y are fairly close to each other on all 3 days, although they use different PBL schemes and LSMs. One possible reason for the large discrepancies between observed and simulated CO is the uncertainty in the CO boundary conditions. For all simulations, boundary conditions for CO are set to be 70 ppb at the top layer and 80 ppb throughout the troposphere. This setting affects the simulation of moderately long-lived species such as CO throughout the upper layers. A sensitivity simulation is conducted using a CO boundary condition of 120 ppb throughout the troposphere. The results show improved CO mixing ratios aloft (figure not shown). Similar performance by the four simulations at a level above 1000 m can be attributed to the same CO boundary conditions used for upper layers.

Extremely high mixing ratios of NO and NO_2 (4–24.9 ppb and 5–20.6 ppb, respectively) were observed between 945 and 995 m on 28 August and between 0 and 500 m on 30 August. Such abnormally high values are not reproduced by model simulations, likely because of missing of substantial sources of NO_x (e.g., lighting) at this altitude on those days. Although all simulated values deviate significantly at surface and in the PBL, they begin to correspond well with observations as the height increases. During all flight takeoffs,

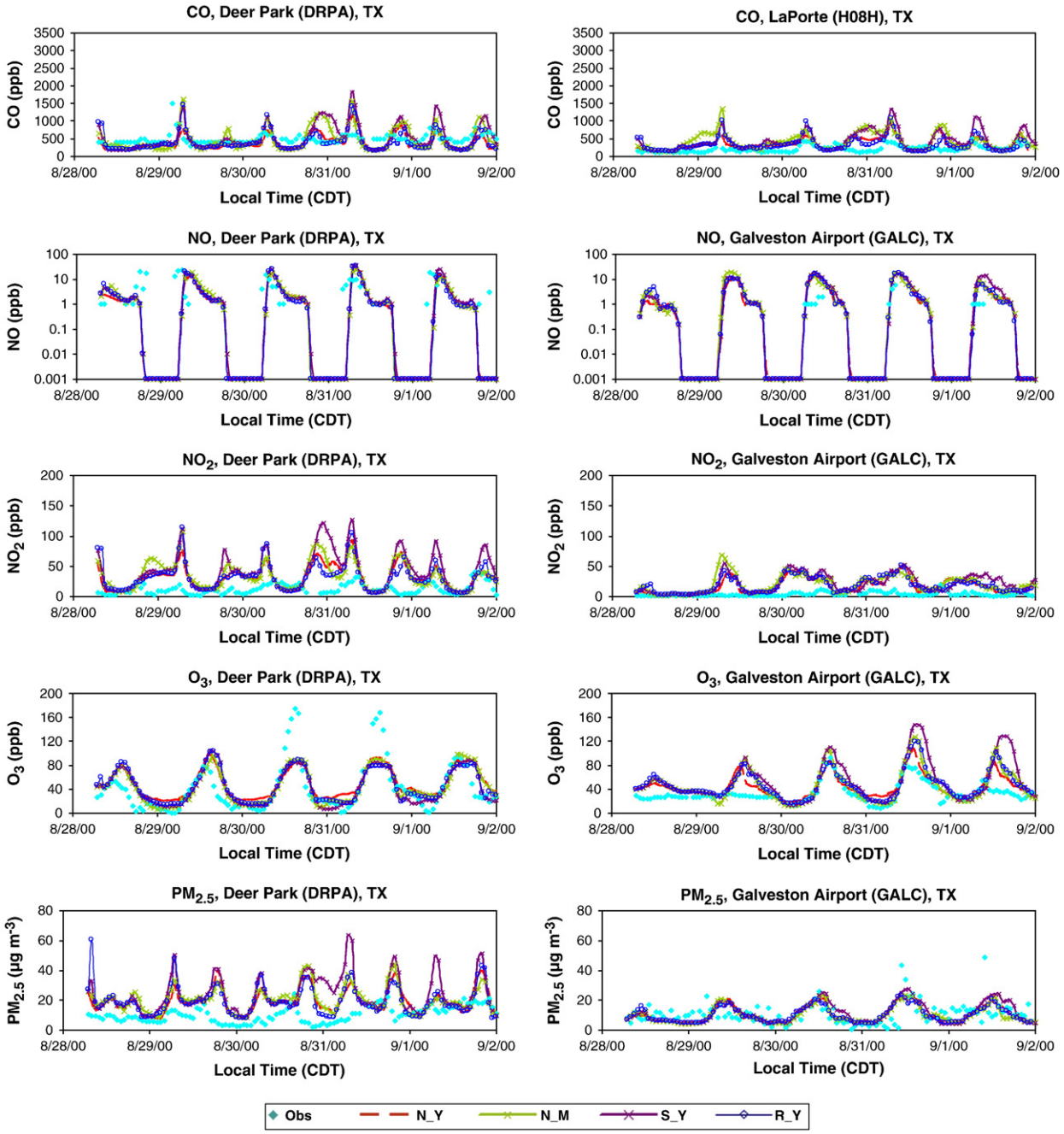

Fig. 7. Observed and simulated time series of CO, NO, NO_2, O_3, and $PM_{2.5}$ from simulations N_Y, N_M, S_Y and R_Y at Deer Park (DRPA), Galveston Airport (GALC) and LaPorte (CO only) (H08H), TX.

simulated values become zero or near zero just above 500 m (except for those abnormally high values), consistent with observations. Compared with N_Y, N_M gives higher NO_x mixing ratios at surface and in the PBL, consistent with temporal analyses shown in Section 3.1.2.2. Larger differences exist between S_Y and other simulations, with the largest differences occurring on 1 September. S_Y simulates a much slower decrease in the NO_2 mixing ratios up to a level of 1000 m as compared with N_Y and R_Y.

Low O_3 mixing ratios were observed between 945 and 995 m on 28 August and between 0 and 500 m on 30 August, due to its titration by extremely high NO_x mixing ratios. While all four simulations predict variations of O_3 mixing ratios with heights reasonably well on 28 August, large deviations in terms of both magnitudes and variation trends exist between simulated and observed values on 30 August and 1 September and among simulated profiles on 1 September. All four simulations give much higher O_3 mixing

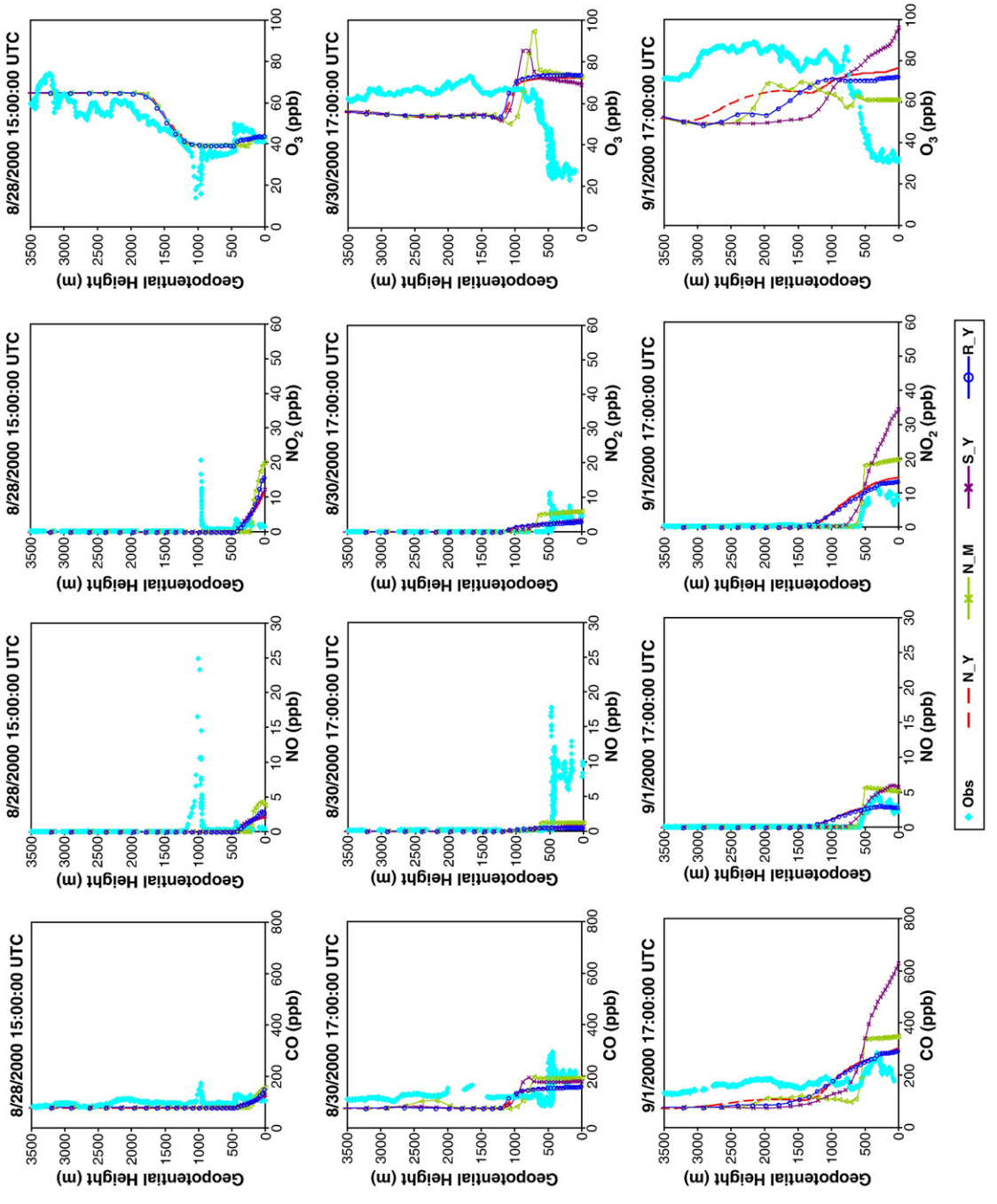

Fig. 8. Observed and simulated vertical profiles of CO, NO, NO_2, and O_3 from simulations N_Y, N_M, S_Y, and R_Y. Observational data are taken from the NOAA's Electra aircraft instrumentation during three flight takeoffs at 15 UTC, August 28, 17 UTC, August 30, and 17 UTC, September 1, 2000.

ratios than observations at surface and below ~700 m. Compared with N_Y, N_M gives stronger vertical variability in the magnitude of the gradient relative to height (i.e., dc/dz). This is perhaps due to the effect of local closure used in MYJ vs. non-local closure employed by YSU. Vertical distribution of O_3 in N_Y may be more averaged over several layers as opposed to mixing layer-by-layer as the height increases (Alapaty and Mathur, 1998). The pattern demonstrated by N_M may appear to be a more realistic, as the vertical variations are more indicative of those observed on 1 September, despite inaccuracies in simulated magnitudes. While R_Y gives similar O_3 vertical profiles to N_Y, those simulated by S_Y deviate significantly from N_Y and R_Y on 28 August and 1 September (e.g., S_Y gives much higher O_3 in the PBL than N_Y and R_Y on 1 September).

3.2. Model sensitivity to horizontal grid resolutions and nesting methods

3.2.1. Meteorological predictions

3.2.1.1. Spatial distributions and domain-wide statistics. Fig. 9 shows absolute differences in spatial distributions of T2, RH2, and PBLH between four pairs of simulations: 1W4–1W12, 2W4–2W12, 2W4–1W4, and 2W12–1W12 at 20 UTC (3PM CDT) 30 August 2000. The first two pairs provide the model sensitivity to horizontal grid space using 1- or 2-way nesting, respectively. The last two pairs provide the model sensitivity to nesting method at 4 or 12 km, respectively. While all three variables exhibit a strong sensitivity to horizontal grid space using 1-way nesting and to nesting methods at 4 km, they show relatively small sensitivity to horizontal grid spacing using 2-way nesting and to nesting methods at 12 km. 1W4 gives lower T2 and PBLH by less than 3% and 12–50%, respectively, but higher RH2 by 16–75% than 1W12 over most land areas. 2W4 gives higher T2 and PBLH by 3–13% and 25–100%, respectively, but lower RH2 by 8–40% than 1W4 over most land areas. The differences in the predictions of T2, RH2, and PBLH between 2W4 and 1W4 are much larger than those between 2W12 and 1W12, indicating that the feedbacks from small to large grids via 2-way nesting indeed have higher impacts on the 4-km simulation during the next time step than the 12-km simulation. Similarly, the differences between 1W4 and 1W12 are much larger than between 2W4 and 2W12, indicating that the feedbacks from small to large grids via 2-way nesting diminish some of the sensitivity to the horizontal grid spacing shown in the 1-way nested simulations. Higher sensitivity is found along the costal lines between 1W4 and 1W12 and between 2W4 and 2W12, because the division of land mask and land use does not match exactly with the coastal line when a coarse grid resolution is used and such a division is very sensitive to the grid resolution. Differences in domain-wide statistics are larger in T2, RH2, WD10, U10, and PBLH between 1W4 and 1W12 than between 2W4 and 2W12 and in T2, RH2, and PBLH between 2W4 and 1W4 than between 2W12 and 1W12, consistent with differences in the spatial distributions of each pair of simulation. 1W4 gives the largest cold bias (with an MB of −2.3 °C and an NMB of −7.4%) in T2 but the smallest bias in RH2, WS10, U10, and PBLH among the four simulations. While the results at 4 km show some improvements, the results using 2-way nesting do not show appreciable benefits (they are even worse in some cases). The benefits or disbenefits of 2-way nesting in terms of accuracy and computational efficiency have been reported by other studies. For example, Fast et al. (2006) showed that a simulation with 2-way nesting improved the representation of the urban and point source plumes and the resulting mixing ratios of O_3 and SO_2 within the coarse 12-km domain. Lozej and Bornstein (1999), on the other hand, have shown better performance of MM5 in capturing precipitation using 1-way nesting than 2-way nesting. The poor performance using 2-way nesting may be associated with perturbations to velocities and potential temperature from a nested fine grid to a coarse grid that degrade conservation properties (e.g., energy, enstrophy) required for accurate numerical solutions (Jacobson, 2001) as well as possible mass non-conservation due to the interpolation errors between fine and coarse grids and nonlinearity in chemistry (Fast et al., 2006).

Fig. 10 shows similar difference plots for CO, O_3, and $PM_{2.5}$ between the four pairs of simulations. Similar to meteorological predictions, the chemical predictions show a higher sensitivity to horizontal grid spacing using 1-way nesting than 2-way nesting, and a higher sensitivity to nesting method at 4 km than 12 km, reflecting the impacts of meteorology on chemistry. 1W4 gives higher $PM_{2.5}$ by 6–50% and either higher or lower CO and O_3 than 1W12 over most land areas. 2W4 gives higher O_3 by 8–40%, lower $PM_{2.5}$ by 6–30%, either higher or lower CO than 1W4 over most land areas. Compared with CO that is a primary pollutant with a slow reaction rate, O_3 and $PM_{2.5}$ concentrations are more sensitive to horizontal grid space and nesting methods, because of the nonlinearity involved in their chemical transformation and removal that depend highly on variables that need to be resolved at a small-scale such as cloud formation, land-surface exchange, and land use. Compared with 1W12, the positive effect of lower PBL on O_3 and its precursors (i.e., increase their concentrations) dominates over the negative effect of the lower T2 (i.e., decrease their concentrations) in 1W4, leading to higher O_3 from 1W4 over the Houston and Galveston areas. Both lower T2 and lower PBLH have a positive effect on $PM_{2.5}$, leading to a net increase in $PM_{2.5}$ levels simulated in 1W4. Compared with 1W4, the positive effect of higher T2 on O_3 and its precursors dominates over the negative effect of the higher PBL in 2W4, leading to higher O_3 over most of the 4-km domain. Both higher T2 and higher PBLH will lead to a net decrease in $PM_{2.5}$ concentrations simulated in 2W4. Differences in domain-wide statistics are larger in O_3, NO, NO_2, and $PM_{2.5}$ between 1W4 and 1W12 than between 2W4 and 2W12 and in O_3, NO, NO_2, and CO between 2W4 and 1W4 than between 2W12 and 1W12, consistent with differences shown in their spatial distributions. Among all simulations, 1W4 gives the largest bias in NO_2 but the smallest bias in O_3, NO, and CO; 1W12 gives the largest bias in NO but the smallest bias in NO_2 and $PM_{2.5}$; 2W12 gives the largest bias in O_3; and 2W4 gives the largest biases in CO and $PM_{2.5}$. Similar to meteorological predictions, 2W4 leads to worse performance than either 1W4 or 1W12 in most chemical predictions, for the same reasons stated previously.

The temporal variations of meteorological and chemical variables are sensitive to horizontal grid spacing and nesting

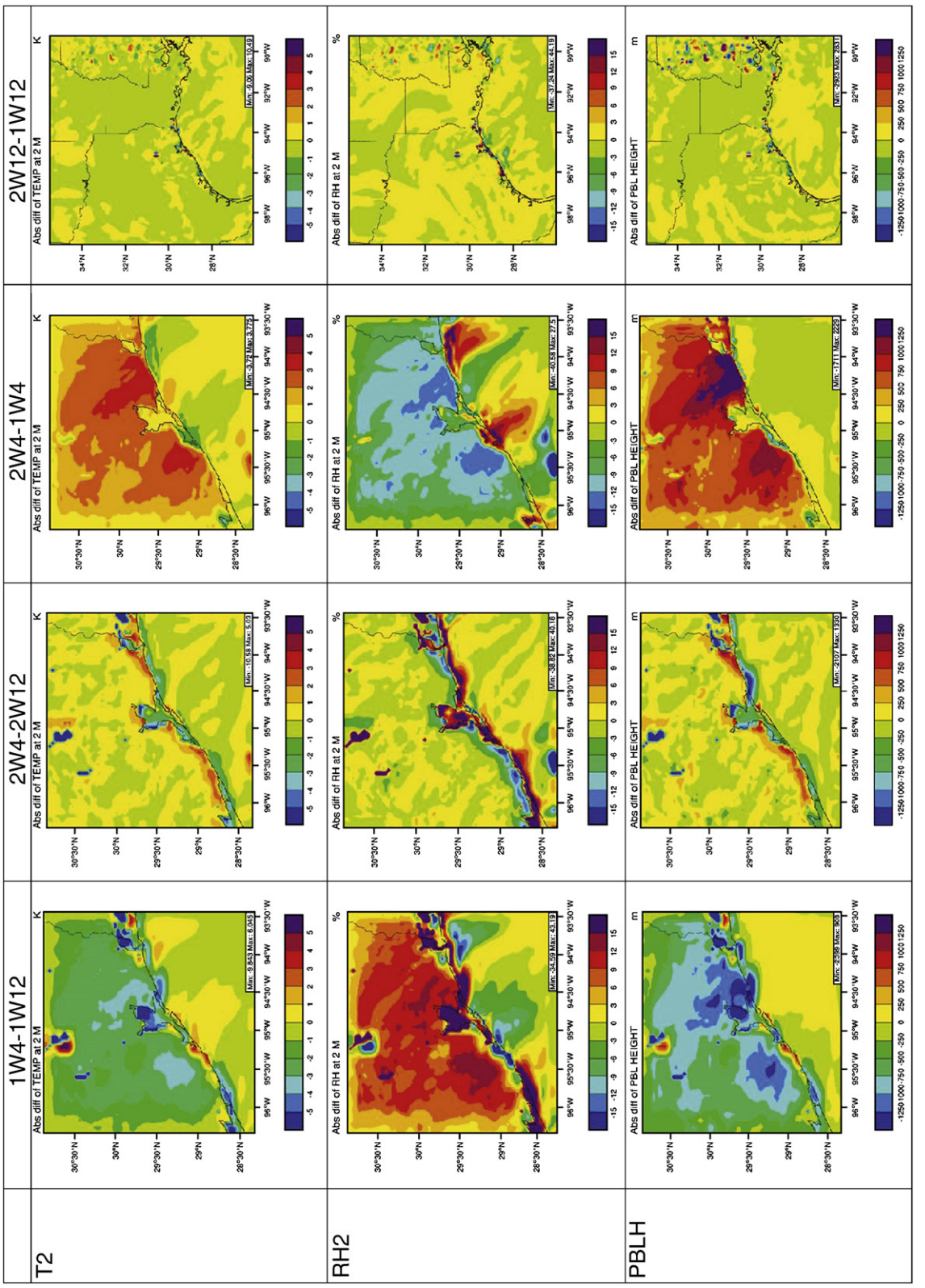

Fig. 9. Absolute differences in spatial distributions of temperature (T2) and relative humidity (RH2) at 2 m and PBL height (PBLH) from simulations 1W12, 1W4, 2W4, and 2W12 at 20 UTC (3PM CDT) 30 August 2000.

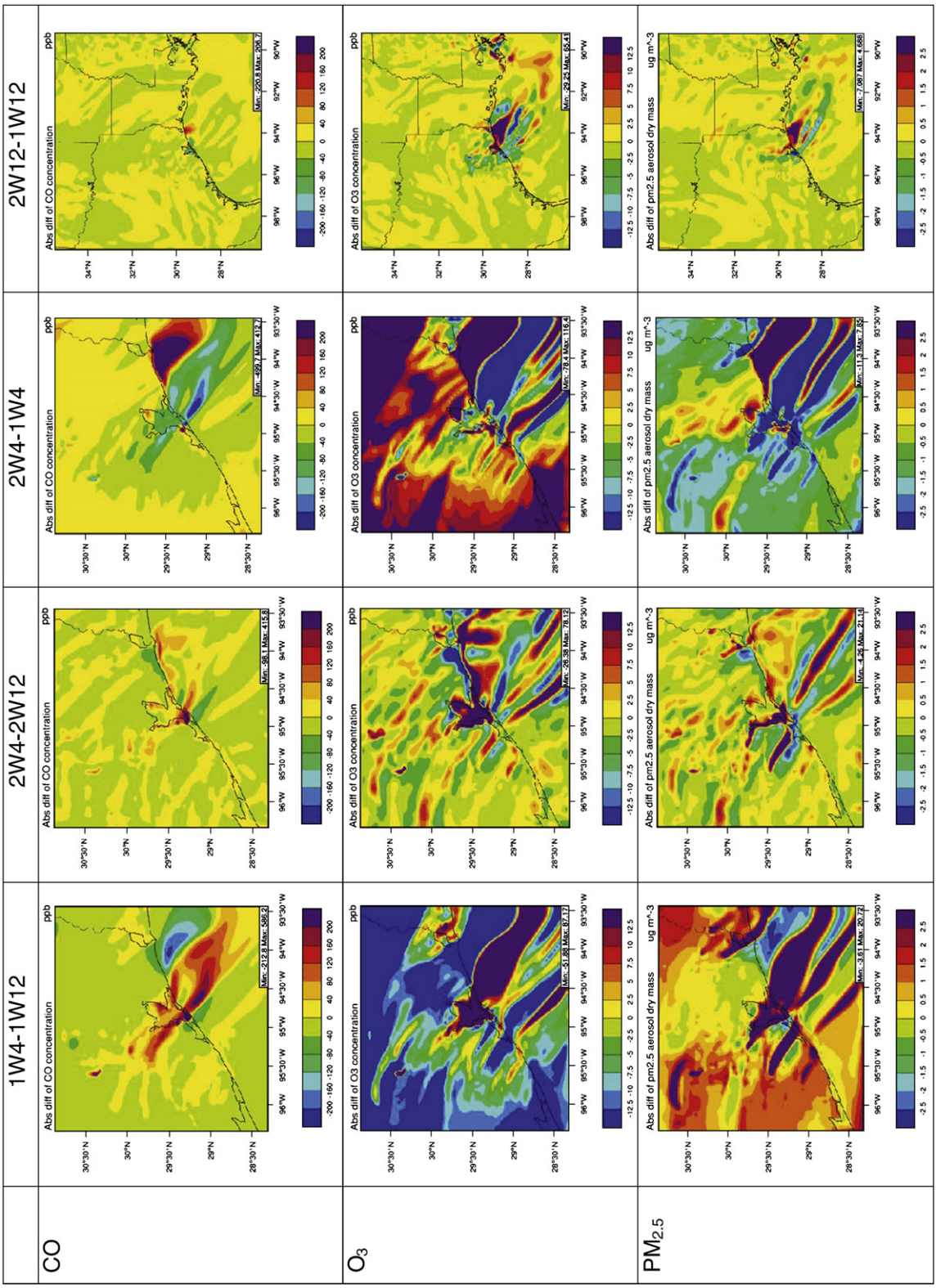

Fig. 10. Absolute differences in spatial distribution of CO, O_3 and $PM_{2.5}$ from simulations 1W12, 1W4, 2W4, and 2W12 on at 20 UTC (3PM CDT) on 30 August 2000.

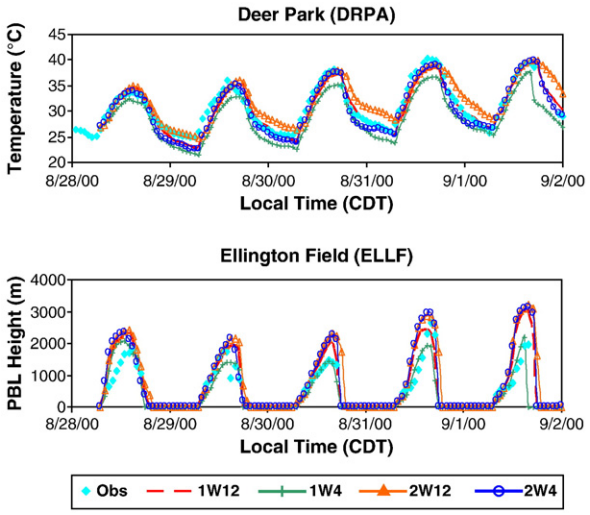

Fig. 11. Observed and simulated time series of temperature at Deer Park (DRPA), TX and PBL height at Ellington Field (ELLF), TX from simulations 1W12, 1W4, 2W12, and 2W4.

methods. As an example, Fig. 11 shows the sensitivity of the simulated temporal profiles of T2 and PBLH at DRPA and Fig. 12 shows similar plots for NO at GALC and O_3 at DRPA. 1W4 gives lower T2 and PBLH than 1W12, and 2W4 gives higher T2 and PBLH than 1W4, consistent with spatial distribution analyses. For T2, the largest sensitivity is found at night and early morning, with the highest values by 2W12 and the lowest values by 1W4. For PBLH, 1W4 gives values that are significantly lower than other simulations but are in better agreement with observations; differences among 1W12, 2W4, and 2W12 are small. Compared with observations, 2W4 gives the best overall agreement for T2 and 1W4 gives the best overall agreement for PBLH at DRPA. Concentrations of primary species such as NO are more sensitive to horizontal grid spacing than nesting methods. For example,

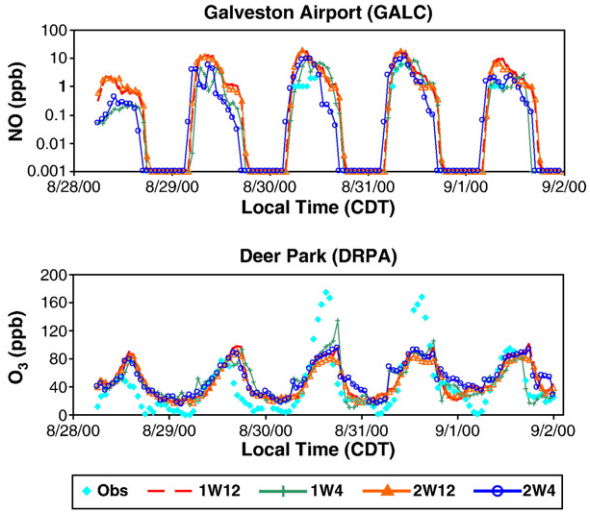

Fig. 12. Observed and simulated time series of NO mixing ratios at Galveston Airport (GALC), TX and O_3 mixing ratios at Deer Park (DRPA), TX from simulations 1W12, 1W4, 2W12, and 2W4.

simulated NO temporal variations are similar between 1W12 and 2W12 and somewhat different between 1W4 and 2W4, but they are largely different between 1W12 and 1W4 and between 2W12 and 2W4 at GALC. The high sensitivity of NO to horizontal grid spacing is due to the importance of grid scale in resolving its emissions and chemical reactions. Compared with 1W12 and 2W12, 1W4 and 2W4 seem to agree relatively better with very limited observations at DRPA on days 3–5. All four simulations give comparable daytime O_3. One exception occurs on 30 August when 1W4 gives much higher O_3 than the other three simulations and also better agreement with observations, indicating that the 4-km resolution helps improve the representation of the urban and point source plume at DRPA because of better representations of emissions and land use. Larger differences exist at night than daytime, with the highest values by 2W4 and the lowest values by 1W4. None of the simulations give sufficient titration by NO_x that leads to lower O_3 mixing ratios at night. They are not able to reproduce the observed peak mixing ratios on 30–31 August. Among the four simulations, 1W4 gives the best overall agreement for O_3. Overall, chemical predictions are highly sensitive to both horizontal grid spacing with 1- or 2-way nesting and to nesting methods at 4 km, with a higher sensitivity to horizontal grid spacing than nesting methods.

4. Summary

This study examines the sensitivity of meteorological and chemical predictions from WRF/Chem to PBL processes, land-surface processes, horizontal grid spacing, and nesting methods for a 5-day summer episode over the Houston–Galveston area in Texas from the TexAQS-2000. Simulations are conducted with four pairs of physics combinations that consist of two PBL schemes (YSU and MYJ) and three land-surface modules (NOAH, Slab, and RUC) (i.e., simulations N_Y, N_M, S_Y, and R_Y) and four sets of configuration combinations that consist of two horizontal grid spacing (4 and 12 km), and two nesting methods (1- and 2-way) (i.e., simulations 1W4, 1W12, 2W4, and 2W12).

Meteorological predictions show small to significant sensitivity to PBL schemes. The two PBL schemes, YSU and MYJ, give overall similar predictions for T2, RH2, WS10, and WD10. PBLH predictions exhibit the largest differences between the simulations with the two PBL schemes, with lower (by 20–40%) values by MYJ, particularly over western Mississippi along the coastline. Compared with available observations, both PBL schemes reproduce well T2, moderately underpredict RH2, and have moderate biases in wind field predictions. N_Y and N_M give moderate to high overpredictions, with better performance for the MYJ PBL scheme. Both schemes have difficulties in reproducing observed T2 and RH2 at a coastal site (i.e., GALC), indicating model deficiencies in capturing small-scale meteorological phenomena under complex weather patterns involving land/sea interactions. Both schemes give similar vertical *T* profiles that match reasonably well with observations but different RH profiles that deviate from observations. Different from the finding of Hong and Pan (1996), non-local closure scheme such as YSU does not always give more accurate *T* and RH in the PBL than local closure scheme such as MYJ.

Larger sensitivity to LSMs is found for all meteorological predictions, due to large differences in simulated latent heat and sensible heat fluxes by these modules. Simulated T2 and PBL heights are the lowest by Slab and the highest by RUC. Simulated RH2 values are the highest by Slab and the lowest by RUC. Such differences can be explained by their different formulations in terms of soil moisture and soil depth treatments. As a result of the simplest treatments and the shallowest soil depth, Slab gives higher latent heat fluxes and lower surface sensible heat fluxes than NOAH and RUC, which in turn affect T2 and PBL height predictions. Compared with observations, S_Y gives the largest cold bias (−1.3 °C) for T2 and R_Y gives the smallest cold bias (−0.1 °C) and the best agreement in diurnal variations. None of the three simulations reproduce observed T2 and RH2 at a coastal site, indicating other factors such as accuracy in land use data may play an important role. Among the three simulations, S_Y gives the lowest bias in WS10, with moderate biases for other simulations. All LSMs give similar biases in WD10. All three LSMs overpredict PBLHs, with the smallest bias by S_Y. Larger differences occur in simulated RH profiles by the three LSMs, with a closer agreement between N_Y and R_Y at most altitudes but appreciable differences among them at some altitudes on some days. S_Y gives *T* and RH vertical profiles that are different from N_Y and R_Y.

Chemical predictions are sensitive to PBL schemes, due mainly to their responses to differences in simulated PBLHs. Compared with YSU, MYJ gives lower PBLHs, leading to higher levels of CO, O_3, and $PM_{2.5}$. Compared with observations, YSU and MYJ reproduce well concentrations of $PM_{2.5}$ but moderately-to-significantly overpredict mixing ratios of O_3 and NO_2, and moderately-to-significantly underpredict those of CO and NO. Both schemes can capture relatively well diurnal variations in CO, NO, and O_3 at a suburban site than at a coastal site, although they fail to reproduce the peak O_3 at the suburban site on 30–31 August. Similar to meteorological predictions, chemical predictions are more sensitive to LSMs. Predictions of PBLHs are the lowest by S_Y and the highest by N_Y, which lead to the highest and the lowest, respectively, concentrations of CO, O_3, and $PM_{2.5}$. While S_Y gives the least domain-wide O_3 overpredictions, it gives the highest bias in $PM_{2.5}$ predictions. N_Y gives the largest domain-wide O_3 predictions but its NMB for $PM_{2.5}$ is the second smallest. All the four simulations give high positive biases in NO_2 and high negative biases in NO due to several factors including uncertainties in NO_x emissions, approximations used in solving nitrogen chemistry, and the poor representation of nocturnal PBL by YSU. While NOAH can capture relatively well diurnal variations in CO, NO, and O_3 at individual sites, Slab and RUC give large deviations in diurnal profiles of CO, NO_2, and O_3 at both sites and $PM_{2.5}$ at the suburban site. Simulated vertical profiles of CO, NO, NO_2, and O_3 are highly sensitive to PBL schemes and LSMs in terms of actual profiles and magnitudes. Compared with N_Y, N_M gives more vertical variability in the magnitude of the O_3 mixing ratio gradient relative to height, due possibly to the effect of local closure used in MYJ as opposed to non-local closure employed by YSU. The O_3 vertical profiles by R_Y are similar to N_Y but those by S_Y deviate significantly from N_Y and R_Y during all flight takeoffs.

Predictions of T2, RH2, and PBLHs exhibit a stronger sensitivity to horizontal grid space using 1-way nesting than 2-way nesting and to nesting methods at 4 km than 12 km. At a suburban site, all four simulations capture diurnal variations of T2 and RH2 but show the largest sensitivity in their magnitudes at night and early morning, with the highest values by 2W12 and the lowest values by 1W4. 1W4 gives PBLHs that are significantly lower than other simulations. O_3 and $PM_{2.5}$ are more sensitive than CO to horizontal grid space and nesting methods, because of the nonlinearity involved in their chemistry and removal processes and their dependence on accurate representations of small-scale meteorological processes. Significant differences exist among the four simulations at a suburban site in simulated diurnal variations of CO, NO_2, O_3 and $PM_{2.5}$, with the strongest variations and the highest magnitudes by 1W4.

The use of more physically-complex meteorological schemes or configurations does not give more accurate results for this particular episode. Compared with the N_Y simulation at 12 km, the use of a 4-km horizontal grid spacing and 1-way nesting improves predictions of NO, O_3, and $PM_{2.5}$ but worsens those for NO_2 and increases CPU from 4.9 to 5.3 h per simulation day. The use of 2-way nesting at 4 and 12 km took 12.9 h per simulation day and does not show appreciable benefits in terms of both accuracy and computational efficacy for this particular episode. The poor performance of 2-way nesting for most meteorological and chemical predictions reinforces a need for further model improvement. One limitation of this study is that the 5-day episode may be too short to show the benefits of 2-way nesting in improving the performance of the coarser grid cells downwind of the nested fine grid cells. More research is obviously needed to evaluate the effects and benefits of nesting for coupled meteorology–chemistry modeling for longer episodes.

Acknowledgements

This work was supported by the National Science Foundation award no. Atm-0348819 and the U.S. EPA-Science to Achieve Results (STAR) program (grant # RD833376). Thanks are due Georg Grell and Steve Peckham, NOAA, for proving WRF/Chem and constructive comments on this manuscript; Jerome Fast, PNNL, for proving model inputs for the 5-day TexAQS-2006 episode and valuable comments on this manuscript; Rahul Zaveri, PNNL, for providing chemical species mapping from CBM-Z to RADM2; Mark Estes, the Texas Commission on Environmental Quality (TCEQ), for providing TCEQ's observational data from TexAQS-2000; and Shao-Cai Yu, the U.S. EPA/NOAA, for providing the FORTRAN script for statistical calculations.

References

Ackermann, I.J., Hass, H., Memmesheimer, M., Ebel, A., Binkowski, F.S., Shankar, U., 1998. Modal aerosol dynamics model for Europe: development and first applications. Atmos. Environ. 32, 2981–2999.

Alapaty, K., Mathur, R., 1998. Effects of atmospheric boundary layer mixing representations on vertical distribution of passive and reactive tracers. Meteor. Atmos. Phys 69, 101–118.

Arunachalam, S., Holland, A., Do, B., Abraczinskas, M., 2006. A quantitative assessment of the influence of grid resolution on predictions of future-year air quality in North Carolina. USA. Atmos. Environ. 40, 5010–5026.

Banta, R.M., Seniff, C.J., Nielsen-Gammon, J., Darby, L.S., Ryerson, T.B., Alvarez, R.J., Sandberg, S.P., Williams, E.J., Trainer, M., 2005. A bad air day in Houston. Bull. Amer. Met. Soc. 86, 657–669.

Bao, J.-W., Michelson, S.A., McKeen, S.A., Grell, G.A., 2005. Meteorological evaluation of a weather-chemistry forecasting model using observations from the TEXAS AQS 2000 field experiment. J. Geophys. Res 110, 1–19.

Bright, D.R., Mullen, S.L., 2002. The sensitivity of the numerical simulation of the Southwest monsoon boundary layer to the choice of PBL turbulence parameterization in MM5. Wea. and Fore. 17, 99–114.

Chen, F., Dudhia, J., 2001a. Coupling an advanced land surface-hydrology model with the Penn State-NCAR MM5 modeling system. Part I: model implementation and sensitivity. Mon. Wea. Rev. 129, 569–585.

Chen, F., Dudhia, J., 2001b. Coupling an advanced land surface-hydrology model with the Penn State-NCAR MM5 modeling system. Part II: preliminary model validation. Mon. Wea. Rev. 129, 587–604.

Daum, P.H., Kleinman, L.I., Springston, S.R., Nunnermacker, L.J., Lee, Y.-N., Weinstein-Lloyd, J., Zheng, J., Berkowitz, C.M., 2004. Origin and properties of plumes of high ozone observed during the Texas 2000 Air Quality Study (TexAQS 2000). J. Geophys. Res. 109. doi:10.1029/2003JD004311.

Dudhia, J., 1996. A Multi-layer Soil Temperature Model for MM5, Preprints, Sixth PSU/NCAR Mesoscale Model Users' Workshop. , pp. 49–50.

Ek, M.B., Mitchell, K.B., Lin, Y., Rogers, B., Grunmann, P., Koren, V., Gayno, G., Tarpley, J.D., 2003. Implementation of NOAH land surface model advances in the National Centers for Environmental Prediction operational mesoscale Eta model. J. Geophys. Res. 108 (D22), 8851.

Fast, J.D., Gustafson Jr., W.I., Easter, R.C., Zaveri, R.A., Barnard, J.C., Chapman, E.G., Grell, G., Peckham, S., 2006. Evolution of ozone, particulates, and aerosol radiative forcing in the vicinity of Houston using a fully coupled meteorology–chemistry–aerosol model. J. Geophys. Res. 111 (D21). doi:10.1029/2005JD006721.

Fritz, B.K., 2003. Measurement and Analysis of Atmospheric Stability in Two Texas Regions. Proceedings of the American Society of Agricultural Engineers/National Agricultural Aviation Association Technical Session, December 6–10, 2003, Reno, Nevada. Paper No. AA03-005.

Gego, E., Hogrefe, C., Kallos, G., Voudouri, A., Irwin, J.S., Rao, S.T., 2005. Examination of model predictions at different horizontal grid resolutions. Env. Fluid. Mech. 5, 63–85.

Grell, G.A., Peckham, S.E., Schmitz, R., McKeen, S.A., Frost, G., Skamarock, W.C., Eder, B., 2005. Fully coupled "online" chemistry within the WRF model. Atmos. Environ. 39, 6957–6975.

Holt, T.R., Niyogi, D., Chen, F., Manning, K., LeMone, M.A., Qureshi, A., 2006. Effect of land–atmosphere interactions on the IHOP 24–25 May 2002 convection case. Mon. Wea. Rev. 134, 113–133.

Hong, S.-Y., Pan, H.-L., 1996. Nonlocal boundary layer vertical diffusion in a medium-range forecast model. Mon. Wea. Rev. 124, 2322–2339.

Hong, S.-Y., Dudhia, J., 2003. Testing of a New Non-local Boundary Layer Vertical Diffusion Scheme in Numerical Weather Prediction Applications, 20th Conference on Weather Analysis and Forecasting/16th Conference on Numerical Weather Prediction. Seattle, WA.

Hong, S., Noh, Y., Dudhia, J., 2006. A new vertical diffusion package with an explicit treatment of entrainment processes. Mon. Wea. Rev 134, 2318–2341.

Hong, S.-Y., Kim, S.-W., Dudhia, J., Koo, M.-S., 2008. Stable Boundary Layer Mixing in a Vertical Diffusion Package, Presented at the 9th Annual WRF Workshop, June 23–27. Boulder, Colorado.

Jacobson, M.Z., 2001. GATOR-GCMM: a global through urban scale air pollution and weather forecast model. 1. Model design and treatment of subgrid soil, vegetation, roads, rooftops, water, sea ice, and snow. J. Geophys. Res. 106, 5385–5402.

Jang, J.-C.C., Jeffries, H.E., Byun, D., Pleim, J., 1995. Sensitivity of ozone to model grid resolution. I: application of high-resolution regional acid deposition model. Atmos. Environ. 29, 3085–3100.

Janjic, Z.I., 2002. Nonsingular Implementation of the Mellor–Yamada Level 2.5 Scheme in the NCEP Meso Model, NCEP Office Note No. 437. (61 pp).

Jiang, G., Fast, J.D., 2004. Modeling the effects of VOC and NO_x emission sources on ozone formation in Houston during the TexAQS 2000 field campaign. Atmos. Environ. 38, 5071–5085.

Jimenez, P., Jorba, O., Parra, R., Baldasano, J.M., 2006. Evaluation of MM5-EMICAT2000-CMAQ performance and sensitivity in complex terrain: high-resolution application to the northeastern Iberian Peninsula. Atmos. Environ. 40, 5056–5072.

Liu, M., Westphal, D.L., 2001. A study of the sensitivity of simulated mineral dust production to model resolution. J. Geophys. Res. 106, 18,099–18,112.

Lozej, C., Bornstein, R.D., 1999. The Importance of Nesting and Initial Conditions: MM5 Application to a Winter Storm, in Preprints of Eighth Conference on Mesoscale Processes. Am. Meteorol. Soc, Bonston, Mass.

Mao, Q., Gautney, L.L., Cook, T.M., Jacobs, M.E., Smith, S.N., Kelsoe, J.J., 2006. Numerical experiments on MM5-CMAQ sensitivity to various PBL schemes. Atmos. Environ. 40, 3092–3110.

Mass, C.F., Ovens, D., Westrick, K., Cole, B.A., 2002. Does increasing horizontal resolution produce more skillful forecasts? Bull. Amer. Meteor. Soc. 407–430.

Mathur, R., Shankar, U., Hanna, A.F., Odman, M.T., McHenry, J.N., Coats Jr., C.J., Alapaty, K., Xiu, A., Arunachalam, S., Olerud Jr., D.T., Byun, D.W., Schere, K.L., Binkowski, F.S., Ching, J.K.S., Dennis, R.L., Pierce, T.E., Pleim, J.E., Roselle, S.J., Young, J.O., 2005. Multiscale Air Quality Simulation Platform (MAQSIP): initial applications and performance for tropospheric ozone and particulate matter. J. of Geophys. Res. 110. doi:10.1029/2004JD004918.

Michalakes, J., Chen, S., Dudhia, J., Hart, L., Klemp, J., Middlecoff, J., Skamarock, W., 2001. Development of a next-generation regional weather forecast model, Devel. Teracomputing, pp. 269–276.

Noh, Y., Cheon, W.G., Hong, S.Y., Raasch, S., 2003. Improvement of the K-profile model for the planetary boundary layer based on large eddy simulation data. Boundary-Layer Meteor 107, 401–427.

Pielke Sr., R.A., 2001. Influence of the spatial distribution of vegetation and soils on the prediction of cumulus convective rainfall. Rev. Geophys. 39, 151–177.

Queen, A., Zhang, Y., 2008. Examining the sensitivity of MM5-CMAQ predictions to explicit microphysics schemes and horizontal grid resolutions. Part III — the impact of horizontal grid resolution. Atmos. Environ. 42, 3869–3881.

Schell, B., Ackermann, I.J., Hass, H., Binkowski, F.S., Ebel, A., 2001. Modeling the formation of secondary organic aerosol within a comprehensive air quality model system. J. Geophys. Res. 106, 28,275–28,293.

Smirnova, T.G., Brown, J.M., Benjamin, S.G., Kim, D., 2000. Parameterization of cold-season processes in the MAPS land-surface scheme. J. Geophys. Res. 105, 4077–4086.

Stockwell, W.R., Middleton, P., Chang, J.S., Tang, X., 1990. The second generation regional acid deposition model chemical mechanism for regional air quality modeling. J. Geophys. Res. 95, 16,343–16,367.

Wert, B.P., Trainer, M., Fried, A., Ryerson, T.B., Henry, B., Potter, W., Angevine, W.M., Atlas, E., Donnelly, S.G., Fehsenfeld, F.C., Frost, G.J., Goldan, P.D., Hansel, A., Holloway, J.S., Hubler, G., Kuster, W.C., Nicks Jr., D.K., Neuman, J.A., Parrish, D.D., Schauffler, S., Stutz, J., Sueper, D.T., Wiedinmyer, C., Wisthaler, A., 2003. Signatures of terminal alkene oxidation in airborne formaldehyde measurements during TexAQS 2000. J. Geophys. Res. 108 (D3), 4104. doi:10.1029/2002JD002502.

Wu, S.-Y., Krishnan, S., Zhang, Y., Aneja, V., 2008. Modeling atmospheric transport and fate of ammonia in North Carolina. Part I. Evaluation of meteorological and chemical predictions. Atmos. Environ. 42, 3419–3436.

Zhang, M.-G., Han, Z.-W., 2007. Evaluation of the Regional Atmospheric Modeling System (RAMS) with Aircraft Observations over East Asia during the Spring of 2001, Presentation at the 6th Annual CMAS Models-3 User's Conference. Research Triangle Park, NC.

Zhang, Y., Hu, X.-M., Wen, X.-Y., Schere, K.L., Jang, C.J., 2007. Simulating Climate–Chemistry–Aerosol–Cloud–Radiation Feedbacks in WRF/Chem. Model Development and Initial Application, Presented at the 6th Annual CMAS Conference, Chapel Hill, NC, October 1–3.

Zhang, Y., Liu, P., Pun, B., Seigneur, C., 2006a. A comprehensive performance evaluation of MM5-CMAQ for the summer 1999 Southern Oxidants Study Episode—Part I. Evaluation protocols, databases and meteorological predictions. Atmos. Environ. 40, 4825–4838.

Zhang, Y., Liu, P., Queen, A., Misenis, C., Pun, B., Seigneur, C., Wu, S.-Y., 2006b. A comprehensive performance evaluation of MM5-CMAQ for the summer 1999 Southern Oxidants Study Episode—Part II. Gas and aerosol predictions. Atmos. Environ. 40, 4839–4855.